Biogeosciences, 21, 5725–5743, 2024
https://doi.org/10.5194/bg-21-5725-2024

Biogeosciences Open Access EGU

Seasonal and spatial pattern of dissolved organic matter biodegradation and photodegradation in boreal humic waters

Artem V. Chupakov[1], Natalia V. Neverova[1], Anna A. Chupakova[1], Svetlana A. Zabelina[1], Liudmila S. Shirokova[1,2], Taissia Ya. Vorobyeva[1], and Oleg S. Pokrovsky[2,3]

[1]Institute of Ecological Problems of the North, N. Laverov Federal Center for Integrated Arctic Research, Nab Severnoi Dviny 23, Arkhangelsk 163000, Russia
[2]Geoscience and Environment Toulouse, UMR 5563 CNRS, University of Toulouse, 14 Avenue Edouard Belin, Toulouse 31400, France
[3]BIO-GEO-CLIM Laboratory, Tomsk State University, 35 Lenina Pr., Tomsk 634050, Russia

Correspondence: Oleg S. Pokrovsky (oleg.pokrovsky@get.omp.eu)

Received: 25 January 2024 – Discussion started: 13 February 2024
Revised: 16 October 2024 – Accepted: 6 November 202 – Published: 20 December 2024

Abstract. Studying the competitive effects of microbial and light-induced transformation of dissolved organic matter (DOM) and trace metals is crucially important for understanding the factors controlling aquatic carbon (C), micronutrient and toxicant transformation in boreal waters. Here we determined the biodegradability and photodegradability of DOM and their effects on the behavior of dissolved trace metals in humic surface waters from the European subarctic: an ombrotrophic peat bog continuum (subsurface water–peatland pool–stream) and a stratified forest lake across seasons. Along the bog water continuum, the biodegradation rate was the highest in subsurface waters and the lowest in the acidic peatland pool. Photodegradation was similar for subsurface waters and the stream but was not detectable in the peatland pool. The waters of the forest lake exhibited a strong seasonal effect of biodegradation, which was the highest in October and the lowest in June. Overall, the biodegradation was capable of removing between 1 % and 7 % of initial dissolved organic carbon (DOC), being the highest in the forest lake in October and in the peatland pool in summer. Photolysis was capable of degrading a much higher proportion of the initial DOC (10 %–25 %), especially in the forest lake during June and the bog stream during July. Only a few trace metals (TMs) were sizably affected by both photodegradation and biodegradation of DOM (Fe, Al, Ti, Nb and light rare-earth elements (REEs)), whereas V, Mn, Co, Cu and Ba were affected solely by biodegradation. A likely mechanism of metal removal was their co-precipitation with coagulating Fe(III) hydroxides. Compared to typical CO_2 emissions from inland waters of the region, biodegradation of DOM can provide the totality of CO_2 evasion from lake water surfaces, whereas biodegradation and photodegradation are not sufficient to explain the observed CO_2 fluxes in the bog water continuum. Overall, these results demonstrated strong spatial and seasonal variability in biodegradation and photodegradation of DOM and organic TM complexes, and we call for the need for a systematic assessment of both processes across seasons with high spatial resolution.

1 Introduction

Organic carbon (OC) processing via metabolic biological (heterotrophic bacteria uptake and respiration) and abiotic physicochemical (photolysis) pathways is considered to be one of the major sources of CO_2 supersaturation in surface waters and related C emissions (Lapierre et al., 2013; Tranvik et al., 2009), and photodegradation vs. biodegradation of dissolved organic matter (DOM) remains poorly quantified (e.g., Groeneveld et al., 2016; Shirokova et al., 2021; Raudina et al., 2022). Given sizable CO_2 emissions in boreal and subarctic waters (Karlsson et al., 2021), together with high concentrations of dissolved organic carbon (DOC) (Cole et al., 2007; Vonk et al., 2015), as well as fast, ongoing and predicted environmental changes in high-latitude aquatic and terrestrial ecosystems (Wauthy et al., 2012; Chaudhary et al.,

2020; Harris et al., 2022), the surface waters of subarctic regions are at the forefront of studies on the biogeochemical cycle of C. Although CO_2 emissions from these waters are significantly lower than those in the 10° S–10° N equatorial belt (e.g., Borges et al., 2015), the magnitude of possible changes in C flux from northern waters to the atmosphere remains much less known. Furthermore, there are still important geographical biases linked to insufficient knowledge of rates and mechanisms of DOC transformation in certain regions. An example is wetland-dominated northern aquatic settings, where high concentrations of soil organic C surrounding the bogs provide high concentrations of DOC but also some related trace metals, whose concentration and migration can be strongly controlled by processes of DOM transformation.

Thorough laboratory and field work on DOM biolability and photolability conducted over the past decades has demonstrated that both phenomena are important, and, depending on environmental setting (nutrient regime, photic layer depth, nature of DOM, etc.), one or the other may dominate overall DOM removal in surface waters (Vachon et al., 2016, 2017; Vähätalo and Wetzel, 2004; Obernosterer and Benner, 2004). In addition to DOM, trace elements (limiting micronutrients, toxicants and geochemical tracers) present in the form of organic and organomineral (Fe, Al) colloids and metal–organic complexes may be subjected to strong transformations during microbiological and photolytic degradations of DOM. This, in turn, may impact the bioavailability, toxicity and export fluxes of trace metals from terrestrial to continental aquatic and finally coastal environments.

Recently, specific attention was devoted to the aquatic systems of permafrost peatlands, given their high vulnerability to climate warming and huge potential for release of soil organic C to surface waters (Vonk et al., 2015; Selvam et al., 2017; Shirokova et al., 2019; Payandi-Rolland et al., 2020; Prijac et al., 2022; Rosset et al., 2022; Taillardat et al., 2022). These studies provided a range of DOM susceptibility to biotic degradation. Thus, between 10 % and 40 % of the DOC in lakes, rivers and soil waters of the boreal zone may be available for bacterial uptake over a time frame of several weeks (Berggren et al., 2010; Roehm et al., 2009). This range is consistent with 14 %–16 % of biodegradable DOC (BDOC) assessed globally (Begum et al., 2022). The necessity for further studies was also indicated, most notably with regard to (i) seasonal aspects, given that the overwhelming majority of available studies were performed during Arctic summer (see discussions in Vonk et al., 2015, and Laurion et al., 2021), and (ii) increased spatial resolution, given that sizable variations of BDOC can be observed within quite short distances of a hydrological continuum (Payandi-Rolland et al., 2020; Raudina et al., 2022). Another poorly known aspect is DOM photolability and biolability across the depth of the water column, especially in seasonally stratified lakes which are subject to spring and autumn overturn.

Based on a compilation of available studies on BDOC and their own research, Vonk et al. (2015) argued that there is a negligible amount of biodegradable DOC in aquatic systems without permafrost. This is, however, contradictory to available assessments on biodegradation of aquatic DOM as a major driver of CO_2 emissions in general (Amaral et al., 2021; Liu and Wang, 2022) and in boreal waters in particular (Ask et al., 2012; Lapierre et al., 2013). Furthermore, among all Arctic rivers, the highest annual (20 %) and winter (ca. 45 %) BDOC was reported for the Ob river, which drains through peatlands with minimal permafrost influence (Wickland et al., 2012). These non-exhaustive examples illustrate a certain inconsistency in current estimations of DOC biodegradability in surface, organic-rich waters of the high latitudes, which precludes quantitative modeling of future C fluxes between land, water and atmosphere in these environmentally important regions. Towards addressing these inconsistences, in this study we chose a typical hydrological continuum in a boreal ombrotrophic bog that is in a glacial lake–ridge complex that includes subsurface water, a small peatland pool in the central part of the bog and an outlet stream. Furthermore, we selected a well-studied, deep, stratified humic lake in the same region (Lake Temnoe; Chupakov et al., 2017), where we sampled surface and deep horizons for incubation experiments. The chosen waters represent subarctic non-permafrost regions that exhibit a sizable organic C pool in their soils and high concentrations of DOC in their surface waters. In contrast to previous studies of permafrost peatlands (Shirokova et al., 2019; Laurion et al., 2021; Payandi-Rolland et al., 2020; Mazoyer et al., 2022), where the main source of DOM is peat or ground vegetation like mosses and lichens, in this highly productive southern taiga region, DOC may be more vulnerable to microbial activity due to the presence of forest leachates (i.e., Don and Kalbitz, 2005; Kalbitz et al., 2003; Kawahigashi et al., 2004; Kiikkilä et al., 2013) and much higher bioproductivity for both the terrestrial and aquatic parts of the lake and river ecosystems.

The first working hypothesis behind our study design is that the DOC-rich subsurface water and deep horizons of the humic lake are mostly sensitive to sunlight impact (Stubbins et al., 2010), and the maximal impact of photodegradation is expected during allochthonous aromatic DOM input (high surface inflow to lakes and bogs in June and October). In contrast, maximal biodegradation of DOM is expected during periods of possible phytoplankton bloom in August, when autochthonous organic material is generated in the water column. A broad importance of DOM biodegradation and photodegradation dynamics is that these processes can contribute to CO_2 emissions from water surfaces, thereby directly controlling the C cycling between the land and the atmosphere. Therefore, the first aim of this study was to relate the measured rates of DOM photodegradation and biodegradation to CO_2 emissions observed in the studied water bodies.

A novelty of the present study is addressing trace metal (TM) partitioning during biodegradation and photodegrada-

tion. The link between DOM and trace elements (TEs) is straightforward: in humic waters of peatlands, most TEs (except probably some alkalis and oxyanions) are strongly (> 80 %) associated with DOM in the form of organic and organomineral (Fe, Al) colloids (Pokrovsky et al., 2005, 2012, 2016). As a result, any DOM transformation processes may directly control the pattern of TEs. On the other hand, some TEs may be photosensitive (Mn, Fe), toxic (Al, Cu, As, Cd, Pb) or act as limiting micronutrients (Zn, Co, Ni, Mo) for the bacteria. Our second working hypothesis here is that removal of DOM via photodegradation or biodegradation will change the partitioning of trace elements which are either (i) strongly bound to DOM, such as divalent transition metals, or (ii) incorporated into organomineral (Fe, Al) colloids, such as trivalent and tetravalent hydrolysates. The TEs of the first group might either remain in solution during photodegradation (and hence not modify their total dissolved concentrations) or be taken up by growing bacteria during biodegradation of TE-bound organic matter (Shirokova et al., 2017a, c). The elements of the second group are capable of co-precipitating with Fe and Al hydroxides (and hence scavenged from the aqueous solution) (e.g., Kopáček et al., 2005, 2006). To test these hypotheses, we examined DOM and related trace-metal biodegradation and photodegradation aiming to assess (1) spatial variations along a hydrological continuum of non-permafrost peatland and different horizons of a neighboring deep stratified lake located in the forest and (2) temporal variability during three main hydrological seasons (high flow in June, baseflow in August and the autumn rainy season in October) in the forest lake. Achieving these objectives should allow for quantifying the relative share of biodegradation and photodegradation on overall DOC and TM removal from surface waters via biotic and physicochemical mechanisms.

2 Materials and methods

2.1 Natural settings of a subarctic bog and a stratified lake

The study site is in the northeastern part of the European boreal zone (Arkhangelsk region) (Fig. 1). The mean annual air temperature is 0 °C, and average annual precipitation is 700 ± 50 mm. The pristine ombrotrophic Ilasskoe Bog is located 30 km SE of Arkhangelsk, and it is a typical lake–ridge complex formed from the last glaciation approximately 10 000 years ago. Its total surface area is 89 km^2, with an average peat thickness of 3 m. The hydrological continuum of Ilasskoe Bog includes subsurface water collected via piezometric measurements of perched groundwater from 2–2.5 m depth (called for brevity "piezometer" below), a small lake (Lake Severnoe) and a stream outlet (Fig. 1). Lake Severnoe, located in the central part of the bog, is a typical peatland pool with an average depth of 1.5 m and a surface area

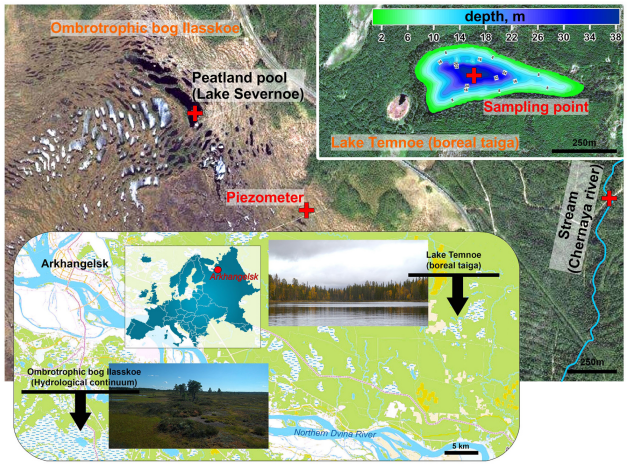

Figure 1. Geographical location of studied hydrological continuum for Ilasskoe Bog waters and deep stratified Lake Temnoe in the boreal forest. Photo and map credits of Artem V. Chupakov.

of 0.013 km^2. Chernyi stream is an outlet for the eastern part of the bog. The stream is 0.7–2.0 m wide and 10 km long, and it flows in a forested (taiga) zone in the shade of the tree canopy. The waters of Ilasskoe Bog are acidic (pH ranges from 3.9–4.0 in piezometer and peatland pool to 5.7 in Chernyi stream), are rich in organics (DOC is equal to 88, 13 and 38 mg L^{-1} in the piezometer, lake and stream, respectively) and have low amounts of minerals (electrical conductivity is 17–46 µS cm^{-1}), as listed in Table 1.

Lake Temnoe is located in a pristine taiga forest 100 km NNE of the town of Arkhangelsk, an area that does not receive any direct anthropogenic impact (Fig. 1). The watershed area is 3.08 km^2, and the lake surface area is 0.091 km^2, with a maximum depth of 37 m and a Secchi disk depth of 3.5 ± 0.5 m. The water residence time in the lake is 394 d. Bogs constitute 31 % of the lake's watershed area, which is represented by carbonate-free loamy moraine atop the peat, podzol and gley soils. The lake water is slightly acidic (pH = 5.1 to 6.0), humic (DOC = 13–20 mg L^{-1}) and dominated by allochthonous DOM with a low concentration of total dissolved ions (electrical conductivity of 20 µS cm^{-1}). Similar to other deep, boreal and subarctic lakes, the lake exhibits two main periods of pronounced stratification (November to April and June to September) and two periods of lake overturn (October and May). Maximal winter stratification occurs in March; the highest water temperature typically occurs in July (see Chupakov et al., 2017, for details). The upper 0–10 m water layer (epilimnion) is not stratified in the course of the year.

The surface waters were collected from the shore (peatland pool and stream) or a PVC boat (Lake Temnoe). Surface (30–50 cm depth) waters were sampled in Ilasskoe Bog, and three water horizons (0.5, 5 and 10 m) were sampled in Temnoe Lake using a pre-cleaned polycarbonate horizontal water

Table 1. Landscape setting, hydrochemical characteristics, and CO_2 concentration and emission fluxes of the studied waters. S.C. is specific conductivity, and EB and OB are eutrophic and oligotrophic bacteria counts, respectively. CFU represents colony-forming unit.

(a) Ilasskoe Bog continuum in July			
	Piezometer	Lake Severnoe	Chernyi stream
GPS coordinates	64.328694° N, 40.612556° E	64.334361° N, 40.609667° E	64.330982° N, 40.653352° E
Description	Shallow groundwater	Peatland pool	Outlet stream
T, °C	11.4	19.4	13
O_2, mg L^{-1}	0.6	8.6	7.5
pH	3.9	4.0	5.7
S.C., µS cm^{-1}	46	17	26
DOC, mg L^{-1}	87.6	12.7	38.4
$SUVA_{254}$	4.13	3.80	4.85
P-PO_4, µg L^{-1}	8.6	3.0	1.7
P_{total}, µg L^{-1}	153	10	20
N-NO_3, µg L−1	111	70	98
N-NH_4, µg L^{-1}	85.4	16.1	12.6
N_{total}, µg L^{-1}	1180	222	399
Si, µg L^{-1}	1808	47	2076
CO_2, µmol L^{-1}	3360	55	318
CO_2 flux, mmol m^{-2} d^{-1}	1600	22	151
EB, CFU mL^{-1}	49 360	56 600	9000
OB, CFU mL^{-1}	54 560	37 900	21 600

(b) Lake Temnoe across seasons and depths									
Month	Jun 0.5	Jun 5	Jun 10	Aug 0.5	Aug 5	Aug 10	Oct 0.5	Oct 6	Oct 10
GPS	64.47683° N, 041.74533° E								
Description	Lake in the northern taiga								
T, °C	12.7	4.9	4.5	18.4	5.5	4.3	9.0	5.8	4.4
O_2, mg L^{-1}	8.45	4.8	4.5	7.78	4.93	2.63	8.90	4.46	2.14
pH	5.2	5.2	5.3	6.0	5.5	5.7	5.2	5.2	5.1
S.C., µS cm^{-1}	17	17	19	17	17	19	18	18	20
DOC, mg L^{-1}	12.6	19.2	21	19	19.5	21.2	19.4	20.6	20.6
$SUVA_{254}$	4.6	4.7	4.6	4.2	4.5	4.5	4.3	4.3	4.7
P-PO_4, µg L^{-1}	2.9	3.3	6.4	0.9	3.6	9.4	3.8	4.6	4.2
P_{total}, µg L^{-1}	19	17	19	20	16	20	18	19	20
N-NO_3, µg L^{-1}	119	150	137	86	152	254	88	85	100
N-NH_4, µg L^{-1}	7.1	8.0	10.0	9.1	17.5	13.8	16.4	14.1	15.5
N_{total}, µg L^{-1}	305	420	408	355	315	337	425	416	396
Si, µg L^{-1}	1940	2268	2354	1183	2208	2714	2269	2380	2380
CO_2, µmol L^{-1}	99	309	329	110	256	337	223	232	253
CO_2 flux, mmol m^{-2} d^{-1}	32	–	–	46	–	–	71	–	–
EB, CFU mL^{-1}	–	36	50	259	92	270	780	220	105
OB, CFU mL^{-1}	50	570	420	–	190	–	680	150	66

sampler (Aquatic Research Co., ID, USA). The water samples were placed into 2 L Milli-Q precleaned PVC jars and kept refrigerated (4 °C) until arrival at the laboratory within 2–3 h of collection.

2.2 Experiments

2.2.1 Biodegradation

For DOM biodegradation assessments, we followed the recommended protocol and used the appropriate type of labware for assessing biodegradable DOC of Arctic waters without external nutrient addition (Vonk et al., 2015; Payandi-Rolland et al., 2020), and we applied a slight modification from Shirokova et al. (2019) to assess maximal possible biodegradation. Initial water samples brought to the laboratory within 2–3 h after sampling were filtered through 3 µm sterilized nylon Sartorius membranes (47 mm diameter); these were used because conventional 0.8–1.2 µm (GF/F) filtration membranes might remove too many microbial cells (Dean et al., 2018).

Duplicate 30 mL aliquots of 3 µm filtered water were placed into pre-combusted (4.5 h at 450 °C) dark borosilicate 40 mL glass bottles wrapped in tinfoil to prevent any photolysis, without nutrient amendment, and incubated at 22 ± 1 °C in the dark. The bottles were closed with loosened sterilized PVC caps to allow for air exchange. The bottles were shaken manually once a day, avoiding cases where the liquid touches the cap. The entire reactor was used for sampling after 0, 2, 5, 8, 12, and 21 d of exposure. Sampled solutions were filtered through sterile, Milli-Q-cleaned Sartorius 0.22 µm filters. The DOC blanks for these filters did not exceed 1 % of DOC concentrations in experimental samples. Sterilized control reactors were filled with natural water that was filtered through a 0.22 µm sterile filter and incubated together with experimental reactors following the approach by Köhler et al. (2002). They were refiltered through 0.22 µm filters of the day of sampling. All handling and sampling of bottles was performed in the laminar flow hood box (class A100) in a sterilized workspace. Filtered samples were acidified with 30 µL of concentrated (8.1 M) double-distilled HCl, tightly capped and stored in the refrigerator before DOC analyses. The non-acidified portion of the filtrate was used for pH, specific conductivity, dissolved inorganic carbon (DIC), and $UV_{254\,nm}$ and optical spectra measurements.

2.2.2 Photodegradation

For photodegradation incubations, water samples were collected in tinfoil-covered pre-cleaned polypropylene jars, sterile filtered (0.22 µm Nalgene Rapid-Flow Sterile Systems) within 2 h of sampling and refrigerated. The filtrates were transferred under a laminar flow hood box into sterilized, acid-washed quartz tubes (150 mL volume, 20 % air headspace) with silicate stoppers and placed at 3 ± 2 cm depth into an outdoor pool which was filled by river water, having light transparency similar to that of Ilasskoe Bog and Temnoe Lake. The outdoor pools were placed in an unshaded area with a latitude similar to the sampling sites (< 30 km from Ilasskoe Bog and Temnoe Lake). Slight wind movement and regular manual shaking allowed for sufficient mixing of reactor interiors during exposure. All photodegradation experiments were run in duplicates. The water temperature (Ebro EBI 20) and light intensity (Luxmeter Testo 545) were continuously recorded every 3 h.

For DOM photodegradation experiments, we followed conventional methods requiring exposure of 0.2 µm sterile filtered samples in quartz reactors to the outdoor pool (Vähätalo et al., 2003; Chupakova et al., 2018; Gareis and Lesack, 2018), to a solar simulator (Lou and Xie, 2006; Amado et al., 2014) or directly to the lake water (Laurion and Mladenov, 2013; Groeneveld et al., 2016). Note that the 0.22 µm sterile filtration is the only way of conducting photodegradation experiments, given that autoclave sterilization of DOM-rich natural waters would coagulate humic material and thereby would not be suitable (Andersson et al., 2018). Filtration through a smaller pore size (i.e., < 0.025 µm), however, would decrease the concentration of DOC and trace metals (i.e., Ilina et al., 2014; Vasyukova et al., 2010). We have chosen a 16 d exposure time for logistical constraints, which is consistent with biodegradation experiments described above and with the duration used in previous studies on photodegradation under sunlight (from 15 to 70 d; Moran et al., 2000; Vähätalo and Wetzel, 2004; Mostofa et al., 2007; Chupakova et al., 2018). Dark control experiments were also conducted in duplicates, using sterilized glass tubes filled with sterile 0.22 µm filtered water, wrapped in tinfoil and placed in the same outdoor pool as the experiments. The headspace (ca. 20 % of total reaction volume) was similar in experimental and control reactors. The individual reactors were sterile sampled at the beginning and after the 0, 2, 5, 8, 12, and 16 d of exposure. The Milli-Q blanks were collected and processed to monitor for any potential sample contamination introduced by our filtration, incubation, handling or sampling procedures. The organic carbon blanks of the filtrates did not exceed 0.2 mg L^{-1}.

2.3 Analyses

The temperature, pH, O_2 and specific conductivity in surface waters were measured in the field. The dissolved CO_2 concentration in the studied bodies of water was measured in situ using a submersible Vaisala Carbocap® GM70 handheld carbon dioxide meter with GMP222 probes (accuracy 1.5 %; see Serikova et al. (2018, 2019) for methodological details). The diffusional CO_2 flux was calculated using a wind-based model (Cole and Caraco, 1998) with $k_{600} = 2.07 + 0.215 \times u_{10}^{1.7}$, where u_{10} is the wind speed at 10 m height, following the approaches developed for surface waters of peatlands (Zabelina et al., 2021). The DOC was an-

alyzed by high-temperature catalytic oxidation using a Shimadzu® total organic carbon analyzer (uncertainty $\pm 2\,\%$, $0.1\,\mathrm{mg\,L^{-1}}$ detection limit) in acidified samples after sparging it with C-free air for 3 min at $100\,\mathrm{mL\,min^{-1}}$ as non-purgeable organic carbon (NPOC). Internationally certified water samples (MISSISSIPPI-03 and Pérade-20) were used to check the validity and reproducibility of the analysis.

The UV and visible (UV–Vis) absorbance of water samples was measured using a 10 mm quartz cuvette on a Cary-50 UV–Vis spectrophotometer to assess the aromaticity of pore fluids via specific UV absorbance ($SUVA_{254}$). In the filtrates, we measured optical density at 254 nm and at selected wavelengths (365, 436, 470, and 665 nm) as well as the entire UV–visible spectrum. The specific UV absorbency ($SUVA_{254}$, $\mathrm{L\,mg^{-1}\,m^{-1}}$) and $E_{470} : E_{665}$ ratios are used as a proxy for the degree of condensation of aromatic groups of DOM (or humification) (Chin et al., 1994; Weishaar et al., 2003; Hur et al., 2006; Peacock et al., 2014). The $E_{254} : E_{436}$ ratio is useful for evaluation of contributions of autochthonous (aquatic) DOM compared to terrestrial (soil) C (Hur et al., 2006; Ilina et al., 2014). The $E_{254} : E_{365}$ ratio also allows for approximating the mean molecular weight of DOM (Hiriart-Baer et al., 2008; Berggren et al., 2007). For better visualization of the differences in spectral parameters between experimental and control reactors, we calculated the difference (ΔA) between the absorbance of the photoreactor or bioreactor and that of the control reactor at each sampling time.

Filtered sampled collected from photodegradation experiments were acidified with ultrapure nitric acid and analyzed for major elements and TEs following the procedures employed by the Geoscience and Environment Toulouse laboratory for analyses of boreal humic waters (Oleinikova et al., 2017, 2018). Major cations, Si, P and ~ 40 TEs were measured with a quadrupole inductively coupled plasma mass spectrometer (ICP-MS) (Agilent 7500ce), using In and Re as internal standards. The international geo-standard SLRS-6 (Riverine Water Reference Material for Trace Metals) was used to check the validity and reproducibility of analyses. Note that for both biodegradation and photodegradation experiments, ICP-MS analyses were performed over 16 d of incubation time.

To check for possible microbial development in biodegradation experiments, we performed oligotrophic and eutrophic bacteria counts over the course of incubation, following the standard methodology used in biodegradation experiments of peat waters (Stutter et al., 2013) and also described previously (Shirokova et al., 2017b; Chupakova et al., 2018). Specifically, an active bacteria number count (colony-forming units, $\mathrm{CFU\,mL^{-1}}$) was performed using petri-dish inoculation (0.1 to 1.0 mL of lake water in three replicates), performed in a laminar flow hood box immediately prior to the experimental incubation start and upon each sampling. Samples were inoculated on nutrient agar ($5\,\mathrm{g\,L^{-1}}$ beef extract, $5\,\mathrm{g\,L^{-1}}$ gelatine peptone, $15\,\mathrm{g\,L^{-1}}$ bacteriological agar; $\mathrm{pH} = 6.8 \pm 0.2$ at 25 °C) to determine the total number of heterotrophic bacteria. Difco@ agar (granulated powder, lot no. 6290083) inoculation was used to assess the number of oligotrophic bacteria. Inoculation of blanks was routinely performed to assure the absence of contamination from external environments.

2.4 Data treatment

The biodegradable and photodegradable DOC and trace metals were calculated as percent loss relative to control, similar to other studies (Vonk et al., 2015; Chupakova et al., 2018; Shirokova et al., 2017b, 2019). However, previous studies in similar environmental contexts of high-DOC humic waters demonstrated that the effects of DOC and element decreases are rather low and often comparable to uncertainties of duplicates (Shirokova et al., 2019). To assess the net effect of biodestruction or photodestruction during the experiment, we used the integral values of concentration change, estimated as the difference between the experiment and the control, while taking into account the standard deviation of replicates. For this, we first calculated the mean of replicates at the ith time of sampling for the experiment and the control of X component ($^{\mathrm{mean}}X_i$ and $^{\mathrm{control}}X_i$, respectively). We next calculated the sum of mean concentration of replicates and its standard deviation ($^{\mathrm{mean}}X_i + \mathrm{SD}_i$). Thus, we obtained three values characterizing the biodegradation or photodegradation process: (1) the change in concentration in the experimental reactor ($^{\mathrm{mean}}\mathrm{S}$), (2) the change in concentration not linked to the studied process ($^{\mathrm{control}}\mathrm{S}$) and (3) the maximal uncertainty of the concentration change in the reactor ($^{\mathrm{mean+SD}}\mathrm{S}$). This allowed for calculating, in percentages, the efficiency of biodegradation or photodegradation of the X component relative to the control, taking into account the relevant uncertainties as follows:

$$X(\%) = 100 \times \left(|^{\mathrm{mean}}X| - |^{\mathrm{control}}X|\right) / |^{\mathrm{control}}X|, \quad (1)$$

$$\mathrm{SD}(\%) = 100 \times \left(|^{\mathrm{mean+SD}}X| - |^{\mathrm{mean}}X|\right) / |^{\mathrm{control}}X|, \quad (2)$$

where X is biodegradable DOC or trace element (BDOC or BTE, respectively) or photodegradable DOC or trace element (PDOC or PTE, respectively). The sign of X designates either a decrease ("−") or an increase ("+") of solute concentration during the experiment. We considered the decrease of concentration significant when $X\,(\%) > \mathrm{SD}\,(\%)$. In other cases, the change was non-systematic over the course of the experiment or non-measurable using the experimental technique employed in the present study.

The mean rate of biodegradation or photodegradation of the X component (V_X) was calculated based on the overall change (ΔX, in %) between the initial (X_0) and final value normalized to overall duration of the experiment t (22 and 16 d for biodegradation and photodegradation, respectively):

$$V_X = (\Delta X / X_0)/t. \quad (3)$$

The SD for rates of component change were calculated in a similar way.

The spectral differences between experimental and control reactors were presented as X–Y–Z diagrams, where X is elapsed time, Y is wavelength and Z is ΔA. The data were plotted in the Surfer software package using triangulation with a linear interpolation method. Statistical treatment included the least-squares method and the Pearson correlation, as the data were normally distributed. All calculations were performed in Statistica version 10 (StatSoft Inc., Tulsa, OK, USA; at $p = 0.05$).

3 Results

3.1 Field-measured C concentration and calculated CO_2 fluxes

The DOC concentration (denoted [DOC]) ranged from 13 to 21 mg L^{-1} in Lake Temnoe, depending on depth and season. The CO_2 concentrations and fluxes increased from June to October and varied from 99 to 337 µmol L^{-1} and 32 to 71 mmol CO_2 m^{-2} d^{-1}, respectively (Table 1). In the Ilasskoe Bog hydrological continuum, the DOC decreased from 88 mg L^{-1} in the peat soil water to 38 mg L^{-1} in the outlet stream. The DOC concentration was generally similar (within ±5 %) between 3, 0.8 (GFF), 0.45 and 0.22 µm pore size filtration of the initial sample, which is in agreement with former size fractionation measurements for Arctic and subarctic systems (Vasyukova et al., 2010; Pokrovsky et al., 2012, 2016; Shirokova et al., 2019). The waters of the Ilasskoe Bog continuum exhibited CO_2 supersaturation with respect to the atmosphere (from 55 to 3300 µmol L^{-1}) and calculated CO_2 emission (diffusion) flux ranged from 22 mmol CO_2 m^{-2} d^{-1} in the peatland pool to 1600 mmol CO_2 m^{-2} d^{-1} in the piezometer (Table 1).

3.2 Biodegradation of DOM

3.2.1 DOC concentration evolution in the experiments

In Temnoe Lake, the range of [DOC] change during the 2–3-week incubation in the experimental reactors did not exceed 2 mg L^{-1} and remained within +0.5 to −1.5 mg L^{-1}, which is less than 10 % of the initial DOC amount (Figs. 2s and Fig. S1 of the Supplement). The biodegradable DOC was both season and depth dependent and ranged from 2 % to 6 % (Table 2). The integral 2-week rates of biodegradation (Table 3, Fig. 3a) demonstrated the highest values during autumn at depths of 0.5 and 10 m and the lowest values during June at all depths. The final 0–10 m water-column- and season-averaged biodegradation rate in Lake Temnoe ranged from 0.02 to 0.04 mg DOC L^{-1} d^{-1}. Rates of biodegradation in the 0–10 m layer demonstrated an increase from May to October, over the entire open water period (Fig. 4a).

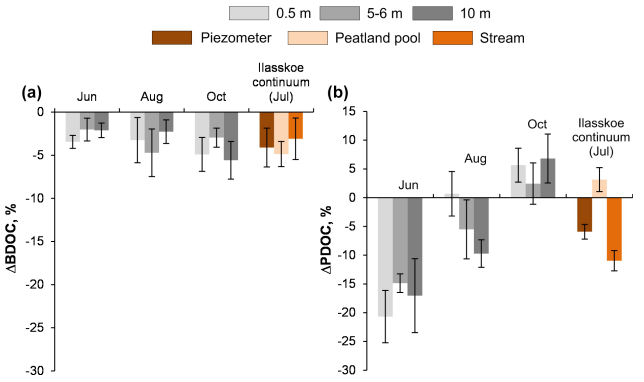

Figure 2. Percentage of biodegradable **(a)** and photodegradable **(b)** DOC presented as relative decrease in DOC concentration between the initial and final values for Temnoe Lake (June, August and October) and Ilasskoe Bog surface waters (July). Error bars are 1 SD of duplicates relative to the control (see Eqs. 1–2 in the text). In accordance with unified protocol of biodegradation experiments (Vonk et al., 2015), positive values signify nil photodegradation (experimental artifacts of DOC production).

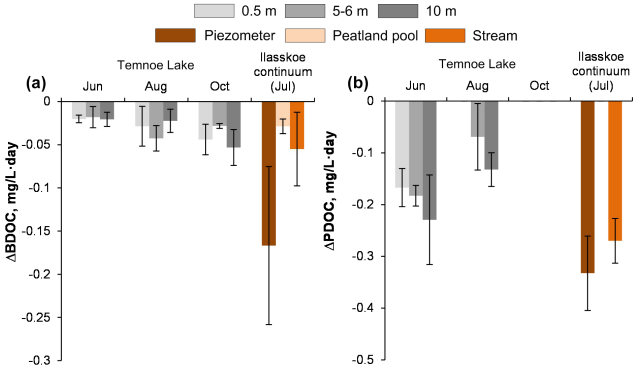

Figure 3. Rates of DOC biodegradation **(a)** and photodegradation **(b)**. The values are negative because they represent a decrease in DOC concentration over the course of the experiment.

For Ilasskoe Bog, the BDOC was highest in the peatland pool (4.9 ± 1.4 %) and lowest in the outlet stream (3.1 ± 2.4 %; Figs. 2a and S1). The integral rate of DOC biodegradation followed the order piezometer ≫ stream > peatland pool and ranged from 0.03 to 0.17 mg C L^{-1} d^{-1} (Table 3, Fig. 3a).

3.2.2 Optical parameters of DOM

In Lake Temnoe, $SUVA_{254}$ remained relatively constant (4.2 to 4.6 L mg C^{-1} m^{-1}) across seasons and depths (Table 1b). Over the course of biodegradation, $SUVA_{254}$ did not change significantly (i.e., less than 0.2 units, which is comparable to the variability of duplicates; Fig. S2). The $E_{254} : E_{436}$ ratio, which is an indicator of humification, increased with incubation time in Lake Temnoe waters; the magnitude of this increase across depth followed the order

https://doi.org/10.5194/bg-21-5725-2024

Table 2. The percent of biodegradable and photodegradable solutes (mean ± SD) whose relative change (concentration decrease) in the course of the experiment was superior to that of SD. Prefixes ΔB and ΔP represent the effect of biodegradation and photodegradation, respectively. Durations of biodegradation and photodegradation are 21.6 ± 0.1 and 15.6 ± 0.1 d, respectively. W represents the probability of measurable effect that is significantly different from changes in the control reactors. Only the components with W ≥ 33 % are presented. Temnoe Lake is a deep stratified lake in a forest. Piezometer, peatland pool and outlet stream represent the hydrological continuum of Ilasskoe Bog.

Index	Temnoe Lake 0.5 m (Jun)	Temnoe Lake 5 m (Jun)	Temnoe Lake 10 m (Jun)	Temnoe Lake 0.5 m (Aug)	Temnoe Lake 5 m (Aug)	Temnoe Lake 10 m (Aug)	Temnoe Lake 0.5 m (Oct)	Temnoe Lake 6 m (Oct)	Temnoe Lake 10 m (Oct)	Piezometer (Jul)	Peatland pool (Jul)	Outlet stream (Jul)
S.C., µS cm^{-1}	17	17	19	17	17	19	18	18	20	46	17	26
ΔB (S.C. ± SD)	−24 ± 4	−26 ± 7	−30 ± 5	−23 ± 3	−27 ± 3	−33 ± 16	−24 ± 7	−23 ± 4	−17 ± 5	0	−18 ± 10	−29 ± 4
DOC, mg L^{-1}	12.6	19.2	21.0	19.0	19.5	21.2	19.4	20.6	20.6	87.6	12.7	38.4
ΔB (DOC ± SD)	3.4 ± 0.8	2.0 ± 1.4	2.1 ± 0.8	3.2 ± 2.6	4.7 ± 1.6	2.3 ± 1.4	4.9 ± 2.0	3.0 ± 0.3	5.6 ± 2.2	4.1 ± 2.3	4.9 ± 1.4	3.1 ± 2.4
ΔP (DOC ± SD)	20.7 ± 4.6	14.9 ± 1.6	17.0 ± 6.4	0	5.5 ± 5.1	9.7 ± 2.4	0	0	0	5.9 ± 1.3	0	11.0 ± 1.8
Al, µg L^{-1}	275	298	329	254	296	335	275	288	323	276	59	388
ΔB (Al ± SD)	3.5 ± 1.4	1.8 ± 0.9	0	2.0 ± 1.3	0	1.4 ± 1.5	2.0 ± 1.9	0	0	0.9 ± 2.2	0	1.3 ± 1.8
ΔP (Al ± SD)	1.9 ± 1.1	2.7 ± 0.9	3.6 ± 1.3	0	2.5 ± 1.3	1.7 ± 2.0	0.7 ± 0.9	0	0	0	0	0.8 ± 0.9
Ti, µg L^{-1}	1.5	2.1	2.6	1.1	2.0	2.6	1.7	1.9	2.5	3.7	0.6	5.0
ΔB (Ti ± SD)	−9.2 ± 1.6	−9.9 ± 7.4	−2.6 ± 2.7	−4.8 ± 3.4	−1.8 ± 2.7	0	−3.6 ± 1.7	−1.0 ± 3.1	−1.0 ± 3.9	−2.3 ± 3.6	−2.2 ± 1.7	−1.4 ± 2.2
ΔP (Ti ± SD)	−-0.1 ± 3	−3 ± 3	−8 ± 3	0 ± 0	−9 ± 1	−3 ± 2	−2 ± 4	0	0	0	−20 ± 4	−3.3 ± 0.5
V, µg L^{-1}	0.5	0.6	0.7	0.4	0.5	0.7	0.4	0.5	0.7	1.1	0.5	1.3
ΔB (V ± SD)	−8.3 ± 16.2	−5.4 ± 3.2	−4.9 ± 2.3	−6.8 ± 7.5	−10.0 ± 4.6	−1.7 ± 1.6	−14.7 ± 11	−13.9 ± 4.3	−16.1 ± 1.7	−3.2 ± 2.6	−0.2 ± 3.4	−17.9 ± 5.0
Mn, µg L^{-1}	39	55	79	17	48	93	30	47	105	78	9	47
ΔB (Mn ± SD)	0	0	−0.3 ± 2.2	−31.8 ± 1.3	−3.2 ± 1.6	−0.6 ± 2.2	−4.8 ± 2.2	−3.2 ± 1.7	−0.4 ± 0.1	0	0	−1.6 ± 2.8
Fe, µg L^{-1}	358	527	710	165	460	795	317	448	820	4402	157	1006
ΔB (Fe ± SD)	−18.1 ± 2.5	−9.1 ± 2.6	−5.4 ± 1.6	−13.5 ± 1.0	−6.3 ± 2.6	−1.4 ± 1.9	−9.5 ± 1.4	−7.8 ± 1.9	−3.3 ± 1.8	−0.8 ± 0.8	−13.6 ± 4.3	−4.5 ± 2.4
ΔP (Fe ± SD)	−3.9 ± 0.6	−2.0 ± 1.9	−4.0 ± 1.3	0	−2.9 ± 1.5	−0.2 ± 0.6	−1.2 ± 0.4	0	0	0	0	0
Co, µg L^{-1}	0.28	0.39	0.68	0.07	0.30	0.65	0.18	0.31	0.74	0.45	0.06	0.30
ΔB (Co ± SD)	−2.2 ± 5.1	−1.2 ± 2.1	−3.7 ± 4.6	−32.7 ± 2.6	−8.1 ± 5.6	−2.7 ± 3.3	−11.0 ± 4.4	−9.1 ± 5.1	−1.6 ± 0.4	0	0	−20.6 ± 27.8
Cu, µg L^{-1}	0.5	0.6	0.7	0.6	0.6	0.7	0.7	0.7	0.5	1.5	0.3	0.8
ΔB (Cu ± SD)	0	0	0	−14.3 ± 1.4	−6.8 ± 4.0	−17.9 ± 11.0	−5.3 ± 4.8	−4.1 ± 8.0	−1.4 ± 12.3	0	−7.7 ± 9.9	0
Ga, µg L^{-1}	0.017	0.022	0.026	0.012	0.016	0.023	0.017	0.015	0.024	0.126	0.016	0.066
ΔP (Ga ± SD)	−14 ± 6	−13 ± 5	−10 ± 4	0	−1 ± 8	0	−10 ± 4	0	0	−7 ± 5	−5 ± 8	−6 ± 3
Y, µg L^{-1}	0.22	0.25	0.28	0.20	0.24	0.28	0.22	0.23	0.28	0.10	0.01	0.21
ΔP (Y ± SD)	−1.3 ± 4.6	−6.7 ± 0.9	−5.3 ± 2.5	0	−2.3 ± 0.7	−1.0 ± 1.6	−1.4 ± 0.2	0	0	0	−5.8 ± 2.7	0
Zr, µg L^{-1}	0.4	0.4	0.5	0.4	0.5	0.5	0.4	0.4	0.5	0.3	0.1	0.4
ΔP (Zr ± SD)	−15 ± 4	−14 ± 0	−13 ± 2	−9 ± 20	−17 ± 1	−14 ± 3	−4 ± 4	0	0	0	−32 ± 3	−8 ± 1
Nb, µg L^{-1}	0.016	0.020	0.025	0.012	0.020	0.024	0.017	0.018	0.025	0.033	0.005	0.042
ΔB (Nb ± SD)	−3.6 ± 10.2	−1.7 ± 7.0	0	−7.7 ± 4.8	−1.1 ± 2.6	0	−7.3 ± 2.3	−1.5 ± 6.3	−5.0 ± 4.0	−2.4 ± 1.5	0	0
ΔP (Nb ± SD)	−9 ± 3	−8 ± 3	−9 ± 1	−6 ± 23	−13 ± 2	−10 ± 5	−8 ± 4	0	−3 ± 3	0	−13 ± 10	−10 ± 4
Ba, µg L^{-1}	4.8	5.1	5.8	4.6	5.0	5.7	4.9	4.8	5.6	54.4	1.5	56.8
ΔB (Ba ± SD)	−2.2 ± 0.7	−2.8 ± 1.7	−1.0 ± 2.7	0	0	0	−1.9 ± 0.5	−1.7 ± 3.7	−5.9 ± 1.6	0	0	−1.3 ± 3.4
La, µg L^{-1}	0.23	0.26	0.30	0.21	0.26	0.32	0.24	0.27	0.31	0.07	0.01	0.22
ΔB (La ± SD)	−4.9 ± 6.5	0	0	−3.9 ± 0.9	−0.3 ± 1.6	−2.6 ± 1.5	−1.1 ± 3.6	−2.4 ± 1.2	−4.0 ± 2.8	−0.8 ± 10.4	−29.7 ± 10.0	−2.0 ± 2.8
ΔP (La ± SD)	−3.8 ± 3.6	−1.2 ± 5.9	−2.0 ± 2.7	0	−3.6 ± 1.0	−3.2 ± 1.6	−1.8 ± 0.9	−2.6 ± 1.0	0	0	−13.5 ± 3.0	0
Ce, µg L^{-1}	0.58	0.65	0.71	0.50	0.62	0.78	0.59	0.63	0.78	0.21	0.03	0.56
ΔB (Ce ± SD)	−5.2 ± 4.2	0	0	−4.4 ± 0.7	−0.1 ± 1.4	−0.8 ± 1.0	−0.9 ± 2.9	−0.8 ± 1.1	−2.2 ± 2.2	0	−9.3 ± 5.9	−2.0 ± 1.9
ΔP (Ce ± SD)	−4.9 ± 1.9	−6.2 ± 1.2	−1.1 ± 1.7	0	−1.5 ± 0.5	−3.2 ± 1.7	−1.9 ± 1.2	0	−0.047 ± 0.46	−3.7 ± 1.5	−2.4 ± 1.6	−3.6 ± 1.1
Pr, µg L^{-1}	0.075	0.085	0.094	0.069	0.082	0.105	0.077	0.084	0.102	0.027	0.005	0.070
ΔB (Pr ± SD)	−1.9 ± 5.2	0	0	−4.0 ± 1.1	0	−0.7 ± 1.3	0	−0.9 ± 1.6	−3.2 ± 2.3	−3.0 ± 1.7	−10.8 ± 8.4	−1.7 ± 2.3
ΔP (Pr ± SD)	−3.0 ± 3.9	−5.5 ± 0.9	−0.4 ± 2.9	13.7 ± 20.8	0	−6.1 ± 2.8	0	−1.3 ± 1.8	0	−0.01 ± 2.4	−16.9 ± 3.0	−2.4 ± 2.1

Table 2. Continued.

Index	Temnoe Lake 0.5 m (Jun)	Temnoe Lake 5 m (Jun)	Temnoe Lake 10 m (Jun)	Temnoe Lake 0.5 m (Aug)	Temnoe Lake 5 m (Aug)	Temnoe Lake 10 m (Aug)	Temnoe Lake 0.5 m (Oct)	Temnoe Lake 6 m (Oct)	Temnoe Lake 10 m (Oct)	Piezometer (Jul)	Peatland pool (Jul)	Outlet stream (Jul)
Nd, $\mu g\,L^{-1}$	0.33	0.34	0.39	0.29	0.33	0.42	0.33	0.32	0.41	0.11	0.02	0.27
ΔP (Nd $\pm$ SD)	-7.8 ± 2.4	-4.5 ± 2.5	-0.8 ± 2.1	0	0	-3.8 ± 2.5	-2.0 ± 3.3	0	0	-2.5 ± 2.8	-24.7 ± 6.2	0
Eu, $\mu g\,L^{-1}$	0.015	0.017	0.016	0.012	0.016	0.020	0.014	0.018	0.021	0.011	0.001	0.017
ΔP (Eu $\pm$ SD)	0	-10.9 ± 3.3	0	0	-0.8 ± 4.7	-3.0 ± 4.0	0	-8.7 ± 8.4	-6.9 ± 4.2	-23.7 ± 8.6	-58.2 ± 15.2	-1.0 ± 1.0
Gd, $\mu g\,L^{-1}$	0.06	0.07	0.08	0.05	0.07	0.08	0.06	0.07	0.09	0.02	0.00	0.06
ΔP (Gd $\pm$ SD)	-0.2 ± 4.4	-6.5 ± 2.9	-3.5 ± 3.5	0	-6.0 ± 3.2	-7.6 ± 1.9	-2.3 ± 2.0	0	-6.7 ± 3.2	0	0	-3.2 ± 3.5
Ho, $\mu g\,L^{-1}$	0.009	0.009	0.011	0.007	0.009	0.011	0.009	0.009	0.011	0.004	0.0004	0.009
ΔP (Ho $\pm$ SD)	-1.9 ± 1.5	-0.3 ± 1.6	-4.6 ± 6.5	0	-0.1 ± 3.6	-3.4 ± 3.2	-11.0 ± 4.9	0	0	-21.5 ± 11.3	0	-10.9 ± 5.5
Er, $\mu g\,L^{-1}$	0.023	0.025	0.033	0.022	0.026	0.030	0.022	0.023	0.031	0.011	0.001	0.023
ΔB (Er $\pm$ SD)	0	0	0	-5.2 ± 3.0	-2.1 ± 1.8	0	-2.1 ± 3.5	0	-2.0 ± 5.3	-15.6 ± 4.9	-22.9 ± 19.5	0
Pb, $\mu g\,L^{-1}$	0.23	0.24	0.23	0.16	0.23	0.39	0.28	0.28	0.32	11	0.35	0.65
ΔB (Pb $\pm$ SD)	0	0	0	-21.3 ± 2.5	-2.0 ± 7.6	-2.4 ± 1.6	-8.2 ± 3.3	-7.2 ± 9.9	-0.8 ± 2.7	0	-17.4 ± 1.0	-8.5 ± 10.9
Th, $\mu g\,L^{-1}$	0.046	0.052	0.066	0.058	0.054	0.064	0.053	0.054	0.061	0.019	0.005	0.050
ΔP (Th $\pm$ SD)	0	0	-11.6 ± 2.6	-12.2 ± 22.5	-7.8 ± 3.2	-18.1 ± 5.6	0	0	-2.0 ± 1.9	0	-49.5 ± 1.3	-10.6 ± 0.8

Table 3. Mean ($\pm$ SD), depth-integrated rates of biodegradation and photodegradation ($mg\,C\,L^{-1}\,d^{-1}$).

Object	$V_{Biodegradation}$	$V_{Photodegradation}$
Lake Temnoe		
Forest lake (Jun)	-0.02 ± 0.0014	-0.19 ± 0.03
Forest lake (Aug)	-0.031 ± 0.010	-0.067 ± 0.066
Forest lake (Oct)	-0.042 ± 0.013	0
Ilasskoe Bog continuum (Jul)		
Piezometer water	-0.17 ± 0.09	-0.33 ± 0.07
Peatland pool	-0.029 ± 0.008	0
Outlet stream (Chernyi)	-0.055 ± 0.043	-0.27 ± 0.043

"0.5 m > 5 m > 10 m" (Fig. S3). The E_{254}/E_{365} ratio also increased over the course of biodegradation, corresponding to an increase of mean molecular weight of DOM (Hiriart-Baer et al., 2008; Berggren et al., 2007). The E_{365}/E_{470} ratio also demonstrated the strongest increase in surface horizons and virtually no change in the deepest horizon (Fig. S3). An increase in the $E_{470} : E_{665}$ ratio corresponds to a decrease in the degree of aromaticity (humification). An increase in the $E_{254} : E_{436}$ ratio signifies a decrease in the contribution of autochthonous (aquatic) DOM compared to terrestrial (soil) C, whereas an increase in the $E_{254} : E_{365}$ ratio characterizes removal of low-molecular-weight compounds.

In Ilasskoe Bog samples, the highest SUVA was observed in the water of the piezometer and the lowest in the stream, but the evolution of this parameter in the course of biodegradation was rather weak (Fig. S3). The $E_{254} : E_{365}$ and $E_{254} : E_{436}$ ratios increased with incubation time in the piezometer and decreased with time in the stream (Fig. S3). The optical ratios ($E_{254} : E_{436}$, $E_{365} : E_{470}$, $E_{470} : E_{665}$) increased in the peatland pool, suggesting an increase in the molecular weight and an increase in the ratio of aromatic to aliphatic compounds.

Complete spectral differences between the experimental and control samples demonstrated rather weak ($\Delta A \leq 0.04$) changes in spectral parameters, mostly detectable after 10–12 d of incubation (Fig. S4). These results were generally consistent with the discrete spectral parameters presented above and demonstrated maximal effects in the piezometer and bog outlet stream. In Lake Temnoe, the maximal impact of biodegradation on spectral parameters was observed in June, at 0.5 m depth.

3.2.3 Bacterial number evolution during biodegradation experiments

The number of cultivable eutrophic bacteria (EB) sizably (ca. 2 orders of magnitude) increased during biodegradation of Lake Temnoe waters. However, this evolution was not systematic in the course of incubation; there was a pronounced

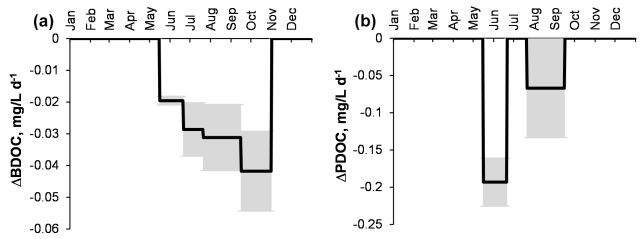

Figure 4. Integral rates of biodegradation (ΔBDOC, **a**) and photodegradation (ΔPDOC, **b**) in the 0–10 m layer of Lake Temnoe across the entire open water period (May to October). Rate values are negative because they signify a decrease in DOC concentration. Note that there was no sampling from December to April and that the photodegradation was not studied in July. Uncertainties are represented by shaded gray rectangles.

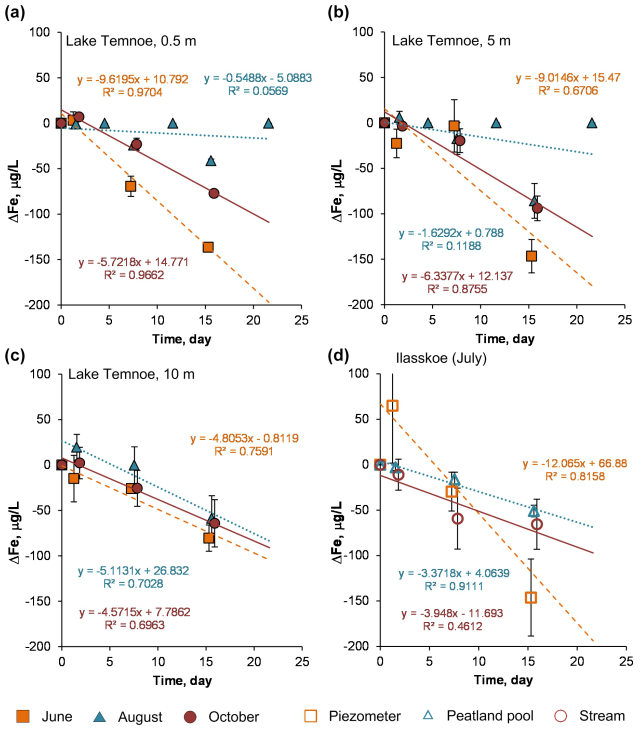

Figure 5. Change in Fe concentration (relative to control) over time in biodegradation experiments. Error bars are 1 SD of duplicates. Temnoe Lake 0.5 m **(a)**, 5 m **(b)** and 10 m **(c)** in June (squares), August (triangles) and October (circles); Ilasskoe Bog continuum in July **(d)** including piezometer (squares), Lake Severnoe peatland pool (triangles) and Chernyi stream (circles).

decrease after 2 weeks of exposure in June and August and a rather stable concentration in waters of all horizons sampled in October (Fig. S5). Such maxima in June and August might be linked to the consumption of substrate or nutrient limitations on bacterial growth. In the Ilasskoe Bog continuum, the number of eutrophic bacteria decreased by an order of magnitude in the peatland pool and piezometer, while it remained constant in the stream. The number of oligotrophic bacteria (OB) increased in waters of all Lake Temnoe horizons by ca. 2 orders of magnitude in August and October and 1 order of magnitude in June. In contrast, the OB number did not change or slightly decreased during incubations of waters from the Ilasskoe Bog continuum (Fig. S5).

3.2.4 Trace element behavior

During biodegradation experiments, a number of trace metals (Group 1) demonstrated a significant ($X >$ SD, Eq. 1) decrease in concentrations across the incubation period (Table 2): Al, Ti, Fe, Co, Cu, Ba, Nb, light rare-earth elements (LREEs) and Pb (as illustrated for Fe in Fig. 5) as well as Mn, V and La (Figs. S6, S7 and S8, respectively). The most significant effects were observed for Fe in the 0–5 m horizon of Lake Temnoe (9 % to 18 % in June, 6 % to 13.5 % in August and 8 % to 9.5 % in October) and 14 % in the peatland pool of Ilasskoe Bog. Overall, for most elements except Fe and Mn, this decease was less pronounced than that of DOC; maximal effects were achieved for Lake Temnoe in August and October (V, Mn, Co, Cu, Ni, Nb, Hf, Pb and Th) and in June (Al and Ti). These elements are typically linked to DOM and Fe and present in the form of organic and organomineral colloids. The second group of major elements and trace elements did not appreciably change their concentration (< 2 % decrease): Li, B, Na, Mg, K, Ca, Si, Ge, As, Rb, Sr, Mo, Sb, Mo and Ba. These elements are not linked to colloids of Fe(III) hydroxide and organic matter. Finally, some elements (Group 3) exhibited unstable behavior without systematic change in concentration during the exposure ($X <$ SD, Eqs. 1–2): Cr, Zn, Cu, Sr, Cd (Y, Zr), Cs, Tl and U. These elements cannot be considered as significantly impacted by the biodegradation process in Lake Temnoe water.

In the Ilasskoe Bog hydrological continuum, the most significant changes during biodegradation were observed in the peatland pool and the outlet stream. Elements strongly (>5 %–10 %; $X >$ SD in Eq. 1) affected by biodegradation were organically or colloidally complexed: V, Fe, Ni, Ga, Y, LREEs and Pb.

3.3 Photodegradation of DOM

3.3.1 DOC concentration evolution

Compared to biodegradation, photodegradation demonstrated much higher values of PDOC and rates of reaction as well as higher variability among seasons and sites. In Lake Temnoe, the PDOC was the highest in June and the lowest in October (Fig. 2b and Table 2). The maximal range of concentration change during the 2-week period achieved 6–8 mg L^{-1} (Fig. S9), which was 10 % to 20 % of the initial [DOC] values. The rates strongly decreased from May–June to the end of summer–autumn. This is consistent with much higher solar radiation in June compared to August and Oc-

tober as measured on site (mean maximal daytime light intensities of 5170 ± 2760, 3220 ± 2160 and 419 ± 176 Lx, respectively). The depth-integrated (0 to 10 m) rates of DOM photodegradation in Lake Temnoe ranged from 0 in October to 0.2 mg C L^{-1} d^{-1} in June (Table 3; Fig. 4b).

In the Ilasskoe Bog hydrological continuum during July, the photodegradation rate followed the order outlet stream > piezometer ≫ peatland pool (Fig. 3b), where integral rates equaled 0.27 ± 0.04, 0.33 ± 0.07, and 0 ± 0.05 mg C L^{-1} d^{-1}, respectively (Table 3).

3.3.2 Optical parameters of DOM

Similar to the DOC concentration, the optical parameters of DOM more strongly evolved over the course of photodegradation compared to the biodegradation experiments. In Temnoe Lake, the strongest decrease in $SUVA_{254}$ was observed in the waters of all horizons in June. This decrease was less pronounced in October (Fig. S10). The $E_{254} : E_{365}$ ratio demonstrated a sizable increase in June, with much weaker increase in October. The $E_{254} : E_{436}$ ratio strongly decreased with exposure time throughout all seasons (10 m depth) and only in June in the surface horizons (Fig. S11). An increase in the $E_{254} : E_{365}$ ratio over the course of photodegradation corresponded to an increase in mean molecular weight of DOM. The $E_{365} : E_{470}$ and $E_{470} : E_{665}$ ratios decreased in all experiments with the Temnoe Lake waters (Fig. S11), suggesting a decrease in the degree of humification (Battin, 1998) and a decrease in the ratio of aromatic to aliphatic moieties.

$SUVA_{254}$ in the Ilasskoe Bog waters remained stable during photodegradation in stream waters and in the piezometer and strongly decreased in the peatland pool (Fig. S10). The $E_{254} : E_{436}$ ratio strongly increased in the peatland pool and exhibited a decrease in stream waters and the piezometer, whereas the $E_{365} : E_{470}$ ratio systematically decreased in all photodegradation experiments with the Ilasskoe Bog continuum (Fig. S11). Finally, the $E_{470} : E_{665}$ ratio exhibited sizable decrease, in the order stream ≫ pool ≥ piezometer. The total spectral differences between experimental and control reactors were mostly pronounced in stratified forest lake waters in June ($\Delta A = -0.4$ to -0.4) and in the bog continuum in July, where effects were strongest in the piezometer and outlet stream waters (ΔA value of -0.4; Fig. S12).

3.3.3 TE in photodegradation experiments

The elements affected by photodegradation also formed three groups, similar to those impacted by biodegradation. Concentrations of Al, Fe, trivalent and tetravalent hydrolysates (Ti, Ga, Zr, Y, LREE and Th), and Nb of Group 1 significantly (> 2 %; $p < 0.05$) decreased during photolysis as illustrated for Fe in Fig. 6 and for Ti and Zr in Figs. S13 and S14, respectively. The decrease of Fe was mostly pronounced in Lake Temnoe water from 10 m depth, whereas decreases of Ti and Zr were detectable for all horizons and seasons except in October. For the Ilasskoe Bog continuum, there was no systematic change in Fe concentration, whereas concentrations of Ti and Zr systematically decreased over the course of sunlight exposure (Figs. S13, S14). Alkali-earth (Li, Rb), alkaline-earth metals (Mg, Ca, Sr, Ba), Si and oxyanions (As, Mo, Sb) of Group 2 were weakly (< 2 %) affected by photolysis. Finally, the remaining trace elements of Group 3 did not exhibit any systematic evolution of concentration during exposure to sunlight, or these changes were inferior to the uncertainties of replicates ($X <$ SD in Eq. 1).

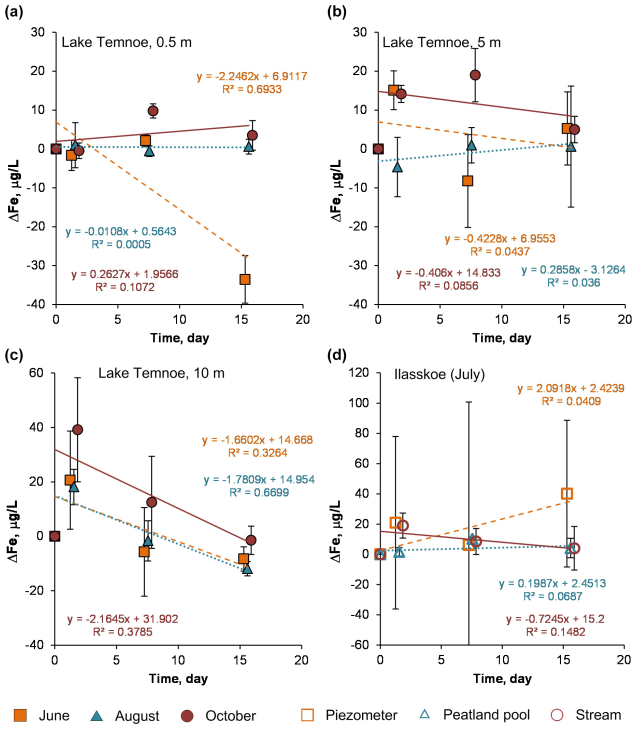

Figure 6. Change in Fe concentration (relative to the control) over time in photodegradation experiments. The error bars are 1 SD of duplicates. Lake Temnoe 0.5 m **(a)**, 5 m **(b)** and 10 m **(c)** in June (squares), August (triangles) and October (circles); the Ilasskoe Bog continuum in July **(d)** includes piezometer (squares), peatland pool Lake Severnoe (triangles) and Chernyi stream (circles).

We found that, unlike for DOC, the magnitude of trace element concentration decrease during photodegradation was generally lower than that of biodegradation experiments. Overall, the strongest effects were observed for Ti (3 % to 9 % in Lake Temnoe; 20 % in Ilasskoe Bog), Ga (6 % to 14 %), Zr (14 %–17 % in Lake Temnoe), Nb (8 % to 13 %) and Th (8 % to 19 % in Temnoe Lake and up to 50 % in Ilasskoe Bog). These effects were mostly pronounced in Temnoe Lake in June and August and in the peatland pool of Ilasskoe Bog (July).

4 Discussion

4.1 Comparison between biodegradation and photolysis

The impact of season on the biodegradable DOC could be tested only for Lake Temnoe because it was sampled during the three main hydrological periods. The maximal biodegradation of the lake water was observed during autumn, when large amount of labile fresh soil organic matter and plant litter were delivered to the lake from the watershed via surface runoff. The water temperature seems to be of secondary importance for the intensity and rate of DOM biodegradation. This is also confirmed by a lack of a statistically significant (at $p < 0.05$) correlation between water temperature and BDOC parameters (overall magnitude and rate). It is worth noting that the seasonal pattern of BDOC in the humic lake quantified in this study (Fig. 4a) contrasted with previous studies on biodegradation of large Arctic streams and rivers whose BDOC decreased as the Arctic summer progressed (Vonk et al., 2015). Presumably, the input of fresh plant litter from the forested watershed of Lake Temnoe provided elevated biodegradation in the water column at the end of the open water season. Another reason could be due to lake overturn in October and exposure of deep, partially autochthonous and thus biodegradable, DOM to the surface horizons. A supply of limiting nutrients (N and P) to the upper 0–10 m layer during lake overturn could also promote such biodegradation in October.

The highest biodegradation rates in the uppermost sections of the bog hydrological continuum (piezometer, Fig. 3a) are consistent with recent findings on organic-rich waters of permafrost peatlands (Shirokova et al., 2019; Payandi-Rolland et al., 2020) and earlier results on headwaters, small streams and soil leachates (Roehm et al., 2009; Ilina et al., 2014; Mann et al., 2014, 2015; Larouche et al., 2015; Spencer et al., 2015; Vonk et al., 2015; Moody et al., 2013; Pickard et al., 2017; Dean et al., 2019). This could be due to the very short water residence time and freshly leached DOM in these water objects (i.e., Mann et al., 2012; Abbott et al., 2014; Payandi-Rolland et al., 2020), given that bioavailable DOM components leached from plant litter are rapidly utilized (Textor et al., 2018). At the same time, overly low BDOC (2 %–8 %) values, regardless of depth and season in the humic lake and across the hydrological continuum of the bog (Fig. 2a), are supportive of previous results for permafrost peatlands from the neighboring region (Shirokova et al., 2019). The general path for DOM spectral property modification over the course of biodegradation consisted of an increase in aromaticity of DOM due to preferential uptake of non-humic low-molecular-weight (LMW) compounds. However, this was not accompanied by a sizable increase in SUVA (Fig. S2). Presumably, the proportion of these compounds in the overall DOC level was quite low and could not impact SUVA evolution. Globally, the evolution of optical ratios was consistent with bacterial consumption of aliphatic LMW compounds and an increase in the overall aromaticity of DOM.

Concerning the seasonal variation of photodegradation in the deep humic lake, maximal effects were observed in June, at the highest solar radiation. These effects likely occurred due to fresh terrestrial organic matter that was leached from the watershed and then efficiently processed during Arctic summer. It should be noted that labile phenolics, carbohydrates, N-containing bases and smaller-molecular-weight compounds are abundant in litter leachates produced during the initial decay stages (Kiikkilä et al., 2011, 2012, 2013; Hensgens et al., 2021). By July, most of the photodegradable DOM was already removed, and in October the effects were much lower. This was consistent with the drastic decrease in sunlight intensity: 5170, 3200 and 420 Lx in June, August and October, respectively, as measured in this study. Therefore, photolabile DOM is delivered from the forested watershed to the lake essentially during surface flux, at high water flow. It is then quickly removed from the water column, which was especially seen in the 0.5 and 5 m horizons of Lake Temnoe. Although labile organic matter from litter was also delivered during the autumn rainy season, presumably, during this period, the conditions for photolysis (low temperature, short daytime period and insufficient light) were not as favorable as those in June or August.

Photodegradation of waters from the Ilasskoe Bog continuum demonstrated maximal rates in the piezometer (Fig. 3b). During photolysis of humic water, a decrease in optical ratios ($E_{365} : E_{470}$; $E_{470} : E_{665}$) clearly indicated preferential degradation of humic aromatic compounds. The strong effect of photodegradation on DOM optical properties in the 500–650 nm region may be linked to decomposition of complex DOM into smaller molecules, whereas a decrease of absorbance in the 230–400 nm region (Fig. S12) indicates degradation of aromatic compounds, progressively increasing over insolation time. A recent study of DOM photolysis in humic-rich forested streams demonstrated that high aromatic material was photochemically converted into smaller non-fluorescent molecules (Wilske et al., 2020).

Results obtained on the more important role of photodegradation over biodegradation are generally consistent with earlier reports on the dominance of photolysis for DOM processing in Arctic waters within North America (Cory et al., 2014; Ward et al., 2017), the Canadian temperate zone (Winter et al., 2007; Porcal et al., 2013, 2014, 2015) and Swedish headwater catchments (Köhler et al., 2002). It is known that DOM photolysis mainly decreases the proportion of aromatic (colored) DOC and produces a rather small (≤ 10 %) change in bulk DOC concentration (Laurion and Mladenov, 2013; Koehler et al., 2014; Groeneveld et al., 2016; Oleinikova et al., 2017; Chupakova et al., 2018; Gareis and Lesack, 2018). The present study corroborates these former findings across a much larger seasonal scale and spatial resolution of boreal surface waters.

As a further perspective of this work, one has to consider biodegradation of photolytically altered DOM given that photo-oxidation is known to transform molecular structures into more bioavailable forms (e.g., Cory and Kling, 2018; Sulzberger et al., 2019), thereby stimulating microbial growth under sunlight, as is known for other Arctic and subarctic settings (i.e., Drozdova et al., 2020; Laurion et al., 2021).

4.2 Possible impact of microbial and photolytic processing on CO_2 emissions from water surfaces

A broad importance of DOM biodegradation and photodegradation dynamics is that these processes can contribute to CO_2 emissions from water surfaces, thereby directly controlling the C cycling between the land and the atmosphere (Lapierre et al., 2013; Tranvik et al., 2009; Cory et al., 2014; Corey an Kling, 2018). In this study, we attempted to relate, for the first time for several diverse aquatic systems across seasons, experimentally measured rates of DOM degradation to in situ-measured CO_2 emissions. The integral rates of DOM bioprocessing in the water column of Lake Temnoe (Table 3, Fig. 4a) allow for quantifying the potential contribution of biodegradation to CO_2 production and emission. Assuming that all biodegraded DOM is transformed into CO_2 and that there is no biomass increase or sedimentation, a 1 m water layer of the lake can emit 1.7 mmol CO_2 m^{-2} d^{-1} in June and 3.3 mmol CO_2 m^{-2} d^{-1} in October. Note that across seasons, Lake Temnoe is not chemically stratified in the first 0–10 m water layer, which does not mix up with anoxic hypolimnion and is not subjected to the influence of sediment respiration (Chupakov et al., 2017). Therefore, integral flux from the 10 m deep water layer amounts to 17–33 mmol CO_2 m^{-2} d^{-1} across the seasons. These values are comparable to typical values of CO_2 evasion from the surface of this lake during different seasons (30–70 mmol CO_2 m^{-2} d^{-1}; Table 1b). For surface waters of Ilasskoe Bog, maximal CO_2 production due to DOM biomineralization alone (Table 3) ranged from 5.0 mmol CO_2 m^{-2} d^{-1} for the peatland pool (2 m deep) to 2.5 mmol CO_2 m^{-2} d^{-1} for the outlet stream (0.5 m deep). However, in summer, the peatland pool and stream emitted 23 and 150 mmol CO_2 m^{-2} d^{-1} (Table 1a), which could not be sustained by DOM biodegradation.

The addition of photodegradation (assuming a photic layer depth of 3.5 m) to DOM bioprocessing in the water column of Temnoe Lake during the open water season can further increase potential CO_2 production in the water column. For the case of Ilasskoe Bog waters, the addition of photolytic degradation increases projected CO_2 emissions from the outlet stream by a factor of 5, which is still below the actual CO_2 flux, whereas DOM photolysis has no impact on CO_2 emissions from the peatland pool. Note that although the depth of sunlight processing in boreal waters is typically 0.8–1.0 m (Vähätalo et al., 2000; Koehler et al., 2014), a more recent study concluded that direct photomineralization of DOM in Arctic humic ponds could be limited to the first centimeters of the water column (Mazoyer et al., 2022). Furthermore, in typical DOM-rich Arctic waters, only half of the sunlight-associated DOC losses are converted to CO_2, and the rest may be turned into particles through photoflocculation (e.g., Mazoyer et al., 2022). Therefore, despite a faster photodegradation rate compared to biodegradation, due to the shallow photic layer in humic waters, the biodegradation may provide the largest impact on CO_2 emissions from the water column of boreal waters.

At the same time, our assumption that all CO_2 in lake water is produced by biodegradation or photodegradation of DOM might not be warranted because there are multiple sources of CO_2 in the lake waters, which were not assessed in the present study. These include but are not limited to particulate organic matter biodegradation and photodegradation, whose importance can strongly exceed that of DOC (e.g., Attermeyer et al., 2018; Lau, 2021; Keskitalo et al., 2022), sediment respiration, plankton and periphyton diel photosynthetic cycle, underground water discharge at the lake bottom, and delivery of DOC- and CO_2-rich waters via lateral surface and shallow subsurface influx. Given that the contribution of each CO_2 source can vary among different water bodies and across seasons, the assessment of DOM biodegradation and photodegradation contribution to overall CO_2 flux in this study should be considered as highly conservative.

4.3 Impact of DOM biodegradation and photodegradation transformation on the trace element pattern

In this study, we hypothesized the following link between DOC and TEs: in humic surface waters of peatlands, most TEs, which include divalent transition metals (Cu, Ni, Co, Zn, Mn), toxicants (Be, Cr, Cd, Pb), trivalent and tetravalent hydrolysates (Al, Ga, Y, REE, Ti, Zr, Hf, Th), except some alkalis and oxyanions, are strongly (> 80 %) associated with DOM in the form of organic, organoferric and organoaluminum colloids (Pokrovsky et al., 2012, 2016). As a result, any DOM transformation processes, be it biodegradation or photodegradation, may directly affect the concentration pattern of TEs. Specifically, the DOM removal via photodegradation or biodegradation should change the speciation of those elements that are strongly bound to DOM such as divalent transition metals or incorporated into organomineral (Fe, Al) colloids, such as trivalent and tetravalent hydrolysates (TE^{3+}, TE^{4+}). The former might either remain in solution during photodegradation (and hence not modify their total dissolved concentrations) or be taken up by growing bacteria during biodegradation. The latter (TE^{3+}, TE^{4+}) are capable of co-precipitating with Fe and Al hydroxides, especially during photodegradation (i.e., Kopáček et al., 2005, 2006) (and hence be sizably removed from the aqueous solution). On the other hand, some TEs are known

to be photosensitive (Mn, Fe), toxic (Al, Cu, As, Cd, Pb) or potentially limiting micronutrients (Zn, Co, Ni, Mo) for the bacteria; therefore, they are capable of affecting the overall rate of photodegradation or biodegradation.

However, contrary to our expectations, among all major elements and trace elements measured in the experiments, only trivalent and tetravalent hydrolysates (TE^{3+}, TE^{4+}) were sizably impacted by both photodegradation and biodegradation. It is known that these elements are essentially present in the form of large molecular size, highly polymerized and presumably aromatic organo-Fe/Al colloids in humic boreal/subarctic lakes (Pokrovsky et al., 2012, 2016), rivers (Krickov et al., 2019; Pokrovsky et al., 2010) and soil porewaters (Pokrovsky et al., 2005; Raudina et al., 2021). Therefore, insoluble TE^{3+} and TE^{4+} generally followed the removal of Fe(III) in the form of particulate Fe hydroxides, after breaking the Fe–DOM bonds that stabilized colloidal Fe(III) hydroxides. This destabilization and Fe hydroxide particle formation process is known to occur either via biodegradation (i.e., Oleinikova et al., 2018) or photolysis (Kopáček et al., 2005, 2006; Oleinikova et al., 2017; Chupakova et al., 2018). At the same time, some micronutrients (V, Mn, Co, Cu and Ba) were affected solely by biodegradation. This can reflect uptake of these metals by growing bacterial cells, as is known from laboratory experiments with pure cultures of heterotrophic bacteria (Shirokova et al., 2017a).

Note that the effects of biodegradation and photodegradation were more pronounced for light REEs (LREEs) compared to heavy REEs (HREEs). This result is consistent with the fact that LREEs have stronger association with Fe hydroxides compared to organic complexes, as known from general chemical considerations and laboratory experiments (i.e., Bau, 1999) as well as evidenced in various boreal and subarctic settings (Pokrovsky et al., 2016; Krickov et al., 2019). Given that the main effect of both photolysis and biodegradation of DOM in humic Fe(III)-rich surface waters is coagulation of dissolved Fe(III) in the form of Fe oxy(hydr)oxides, the LREEs are removed from solution. This removal occurs in the form of adsorbed complexes or coprecipitated Fe oxy(hydr)oxides, while HREEs remain in the form of strong aqueous complexes.

5 Conclusions

Seasonally resolved biodegradability and photodegradability of DOM in a deep stratified lake and summer measurements from a peat bog hydrological continuum within the boreal zone demonstrated that the subsurface and deep horizons of these stratified waters are mostly sensitive to sunlight impact and that the maximal effects of photodegradation occurred in June, during the strongest insolation. In contrast, the biodegradation of DOM from the humic lake was mostly pronounced during October, when fresh leachates of forest litter were exported from the watershed. Insoluble, low-mobility trace metals such as trivalent and tetravalent hydrolysates were affected by both biodegradation and photodegradation, as they are associated with coagulating Fe(III) oxyhydroxides.

A broad implication of the obtained results is that, although DOM photodegradation rates were sizably higher compared to those of biodegradation, the rather thin photic layer in humic waters does not allow for a significant contribution of photolysis in overall CO_2 emissions from lake and bog surfaces. Further work is needed on biodegradation of photolytically altered DOM, given that photo-oxidation is known to transform molecular structures into more bioavailable forms. The high seasonal dynamics and spatial variability in both photodegradability and biodegradability of DOM and related trace elements of humic surface waters in the boreal zone encountered in this study suggest the need for studying these processes during "shoulder seasons" (early spring and late autumn), the periods of maximal photodegradation and biodegradation, respectively. These efforts should be focused on the most dynamic components such as small streams and subsurface waters, which demonstrated the highest rates of both photodegradation and biodegradation.

Data availability. All the data obtained in this work are presented in the Supplement.

Supplement. The supplement related to this article is available online at: https://doi.org/10.5194/bg-21-5725-2024-supplement.

Author contributions. AVC and OSP designed the study and wrote the paper. AAC, NVN and SAZ performed sampling, analyses and interpretations. LSS performed the bacterial number assessments and DOC result interpretations. AVC, TYV and OSP provided analyses of the literature data.

Competing interests. The contact author has declared that none of the authors has any competing interests.

Disclaimer. Publisher's note: Copernicus Publications remains neutral with regard to jurisdictional claims made in the text, published maps, institutional affiliations, or any other geographical representation in this paper. While Copernicus Publications makes every effort to include appropriate place names, the final responsibility lies with the authors.

Acknowledgements. We are grateful to associate editor Koji Suzuki and three anonymous reviewers for insightful and constructive comments.

Financial support. This research has been supported by the Russian Science Foundation (grant no. 22-17-00253) and the Agence Nationale de la Recherche (grant no. ANR-22-PEXF-0011). Publisher's note: the article processing charges for this publication were not paid by a Russian or Belarusian institution.

Review statement. This paper was edited by Koji Suzuki and reviewed by four anonymous referees.

References

Abbott, B. W., Larouche, J. R., Jones, J. B., Bowden, W. B., and Balser, A. W.: Elevated dissolved organic carbon biodegradability from thawing and collapsing permafrost, J. Geophys. Res., 119, 2049–2063, https://doi.org/10.1002/2014JG002678, 2014.

Amado, A. M., Cotner, J. B., Cory, R. M., Edhlund, B. L., and McNeill, K.: Disentangling the interactions between photochemical and bacterial degradation of dissolved organic matter: amino acids play a central role, Microb. Ecol., 69, 554–566, https://doi.org/10.1007/s00248-014-0512-4, 2014.

Amaral, V., Ortega, T., Romera-Castillo, C., and Forja, J.: Linkages between greenhouse gases (CO_2, CH_4, and N_2O) and dissolved organic matter composition in a shallow estuary, Sci. Total Environ., 788, 147863, https://doi.org/10.1016/j.scitotenv.2021.147863, 2021.

Andersson, M. G. I., Catalán, N., Rahman, Z., Tranvik, L. J., and Lindström, E. S.: Effects of sterilization on dissolved organic carbon (DOC) composition and bacterial utilization of DOC from lakes, Aquat. Microb. Ecol., 82, 199–208, https://doi.org/10.3354/ame01890, 2018.

Ask, J., Karlsson, J., and Jansson, M.: Net ecosystem production in clear-water and brown-water lakes, Glob. Biogeochem. Cy., 26, GB1017, https://doi.org/10.1029/2010GB003951, 2012.

Attermeyer, K., Catalán, N., Einarsdottir, K., Freixa, A., Groeneveld, M., Hawkes, J., Bergquist, J., and Tranvik, L. J.: Organic carbon processing during transport through boreal inland waters: Particles as important sites, J. Geophys. Res.-Biogeosci., 123, 2412–2428, https://doi.org/10.1029/2018jg004500, 2018.

Bau, M.: Scavenging of dissolved yttrium and rare earths by precipitating iron oxyhydroxide:experimental evidence for Ce oxidation, Y-Ho fractionation, and lanthanide tetrad effect, Geochim. Cosmochim. Ac., 63, 67–77, https://doi.org/10.1016/S0016-7037(99)00014-9, 1999.

Battin, T. J.: Dissolved organic materials and its optical properties in a blackwater tributary of the upper Orinoco River, Venezuela, Organ. Geochem., 28, 561–569, https://doi.org/10.1016/S0146-6380(98)00028-X, 1998.

Begum, M. S., Park, J.-H., Yang, L., Shin, K. H., and Hur, J.: Optiacl and molecular indices of dissolved organic matter for estimating biodegradability and resulting carbon dioxide production in inland waters: A review, Water Res., 228, 119362, https://doi.org/10.1016/j.watres.2022.119362, 2022.

Berggren, M., Laudon, H., and Jansson, M.: Landscape regulation of bacterial growth efficiency in boreal freshwaters, Global Biogeochem. Cy., 21, GB4002. https://doi.org/10.1029/2006GB002844, 2007.

Berggren, M., Laudon, H., Haei, M., Ström, L., and Jansson, M.: Efficient aquatic bacterial metabolism of dissolved low-molecular-weight compounds from terrestrial sources, ISME J., 4, 408–416, https://doi.org/10.1038/ismej.2009.120, 2010.

Borges, A., Darchambeau, F., Teodoru, C., Marwick, T. R., Tamooh, F., Geeraert, N., Omengo, F. O., Guérin, F., Lambert, Th., Morana, C., Okuku, E., and Bouillon, S.: Globally significant greenhouse-gas emissions from African inland waters, Nat. Geosci., 8, 637–642, https://doi.org/10.1038/ngeo2486, 2015.

Chaudhary, N., Westermann, S., Lamba, S., Shurpali, N., Sannel, A. B. K., Schurgers, G., Miller, P. A., and Smith, B.: Modelling past and future peatland carbon dynamics across the pan- Arctic, Glob. Change Biol., 26, 4119–4133, https://doi.org/10.1111/gcb.15099, 2020.

Chin, Y.-P., Aiken, G., and O'Loughlin, E.: Molecular weight, polydispersity, and spectroscopic properties of aquatic humic substances, Environ. Sci. Technol., 28, 1853–1858, https://doi.org/10.1021/es00060a015, 1994.

Chupakov, A., Ershova, A., Moreva, O. Yu, Shirokova, L. S., Zabelina, S. A., Vorobieva, T. Ya., Klimov, S. I., Brovkon N., and Pokrovsky, O. S.: Seasonal dynamics of dissolved carbon in contrasting stratified lakes of the subarctic, Boreal Environ. Res., 22, 213–230, https://www.borenv.net/BER/archive/pdfs/ber22/ber22-213-230.pdf (last access: 18 December 2024), 2017.

Chupakova, A. A., Chupakov, A. V., Neverova, N. V., Shirokova, L. S., and Pokrovsky, O. S.: Photodegradation of river dissolved organic matter and trace metals in the largest European Arctic estuary, Sci. Total Environ., 622–623, 1343–1352, https://doi.org/10.1016/j.scitotenv.2017.12.030, 2018.

Cole, J. J. and Caraco, N.: Atmospheric exchange of carbon dioxide in a low-wind oligotrophic lake measured by the addition of SF6, Limnol. Oceanog., 43, 647–656, https://doi.org/10.4319/lo.1998.43.4.0647, 1998.

Cole, J. J., Prairie, Y. T., Caraco, N. F., McDowell, W. H., Tranvik, L. J., Striegl, R. G., Duarte, C. M., Kortelainen, P., Downing, J. A., Middelburg, J. J., and Melack, J.: Plumbing the global carbon cycle: Integrating inland waters into the terrestrial carbon budget, Ecosystems, 10, 172–185, https://doi.org/10.1007/s10021-006-9013-8, 2007.

Cory, R. M. and Kling, G. W.: Interactions between sunlight and microorganisms influence dissolved organic matter degradation along the aquatic continuum, Limnol. Oceanogr. Lett., 3, 102–116, https://doi.org/10.1002/lol2.10060, 2018.

Cory, R. M., Ward, C. P., Crump, B. C., and Kling, G. W.: Sunlight controls water column processing of carbon in arctic fresh waters, Science, 345, 925–928, https://doi.org/10.1126/science.1253119, 2014.

Dean, J. F., van Hal, J. R., Dolman, A. J., Aerts, R., and Weedon, J. T.: Filtration artefacts in bacterial community composition can affect the outcome of dissolved organic matter biolability assays, Biogeosciences, 15, 7141–7154, https://doi.org/10.5194/bg-15-7141-2018, 2018.

Dean, J. F., Garnett, M. H., Spyrakos, E., and Billett, M. F.: The potential hidden age of dissolved organic carbon exported by peatland streams, J. Geophys. Res.-Biogeosci., 124, 328–341, https://doi.org/10.1029/2018JG004650, 2019.

Don, A. and Kalbitz, K.: Amount and degradability of dissolve dorganic carbon from foliar litter at different de-

composition stages, Soil Biol. Biochem., 37, 2171–2179, https://doi.org/10.1016/j.soilbio.2005.03.019, 2005.

Drozdova, O. Y., Aleshina, A. R., Tikhonov, V. V., Lapitskiy, S. A., and Pokrovsky, O. S.: Coagulation of organo-mineral colloids and formation of bioavailable low molecular weight organic complexes in boreal humic river water under UV-irradiation, Chemosphere, 250, 126216, https://doi.org/10.1016/j.chemosphere.2020.126216, 2020.

Gareis, J. A. L. and Lesack, L. F. W.: Photodegraded dissolved organic matter from peak freshet river discharge as a substrate for bacterial production in a lake-rich great Arctic delta, Arct. Sci., 4, 557–583, https://doi.org/10.1139/AS-2017-0055, 2018.

Groeneveld, M., Tranvik, L., Natchimuthu, S., and Koehler, B.: Photochemical mineralisation in a boreal brown water lake: considerable temporal variability and minor contribution to carbon dioxide production, Biogeosciences, 13, 3931–3943, https://doi.org/10.5194/bg-13-3931-2016, 2016.

Harris, L. I., Richardson, K., Bona, K. A., Davidson, S. J., Finkelstein, S. A., Garneau, M., McLaughlin, J., Nwaishi, F., Olefeldt, D., Packalen, M., Roulet, N. T., Southee, F. M., Strack, M., Webster, K. L., Wilkinson, S. L., and Ray, J. C.: The essential carbon service provided by northern peatlands, Front. Ecol. Environ., 20, 222–230, https://doi.org/10.1002/fee.2437, 2022.

Hensgens, G., Lechtenfeld, O. J., Guillemette, F., Laudon, H., Berggren, M.: Impacts of litter decay on organic leachate composition and reactivity, Biogeochemistry 154, 99–117, https://doi.org/10.1007/s10533-021-00799-3, 2021.

Hiriart-Baer, V. P., Diep, N., and Smith, R. E. H.: Dissolved organic matter in the Great Lakes: role and nature of allochthonous material, J. Great Lakes Res., 34, 383–394, https://doi.org/10.3394/0380-1330(2008)34[383:DOMITG]2.0.CO;2, 2008.

Hur, J., Williams, M. A., and Schlautman, M. A.: Evaluating spectroscopic and chromatographic techniques to resolve dissolved organic matter via end member mixing analysis, Chemosphere, 63, 387–402, https://doi.org/10.1016/j.chemosphere.2005.08.069, 2006.

Ilina, S. M., Drozdova, O. Yu., Lapitsky, S. A., Alekhin, Yu. V., Demin, V. V., Zavgorodnaya, Yu. A., Shirokova, L. S., Viers, J., and Pokrovsky, O. S.: Size fractionation and optical properties of dissolved organic matter in the continuum soil solution-bog-river and terminal lake of a boreal watershed, Org. Geochem., 66, 14–24, https://doi.org/10.1016/j.orggeochem.2013.10.008, 2014.

Kalbitz, K., Schmerwitz, J., Schwesig, D., and Matzner, E.: Biodegradation of soil-derived dissolved organic matter as related to its properties, Geoderma, 113, 273–291, https://doi.org/10.1016/S0016-7061(02)00365-8, 2003.

Karlsson, J., Serikova, S., Rocher-Ros, G., Denfeld, B., Vorobyev, S. N., and Pokrovsky, O. S.: Carbon emission from Western Siberian inland waters, Nat. Commun., 12, 825, https://doi.org/10.1038/s41467-021-21054-1, 2021.

Kawahigashi, M., Kaiser, L., Kalbitz, K., Rodionov, A., and Guggenberger, G.: Dissolved organic matter in small streams along a gradient from discontinuous to continuous permafrost, Global Change Biol. 10, 1576–1586, https://doi.org/10.1111/j.1365-2486.2004.00827.x, 2004.

Keskitalo, K.H., Bröder, L., Jong, D., Zimov, N., Davydova, A., Davydov, S., Tesi, T., Mann, P. J., Haghipour, N., Eglinton, T. I., and Vonk, J. E.: Seasonal variability in particulate organic carbon degradation in the Kolyma River, Siberia, Environ. Res. Lett., 17, 034007, https://doi.org/10.1088/1748-9326/ac4f8d, 2022.

Kiikkilä, O., Kitunen, V., and Smolander, A.: Properties of dissolved organic matter derived from silver birch and Norway spruce stands: Degradability combined with chemical characteristics, Soil Biol. Biochem. 43, 421–430, https://doi.org/10.1016/j.soilbio.2010.11.011, 2011.

Kiikkilä, O., Kitunen, V., Spetz, P., and Smolander, A.: Characterization of dissolved organic matter in decomposing Norway spruce and silver birch litter, European J. Soil Sci., 63, 476–486, https://doi.org/10.1111/j.1365-2389.2012.01457.x, 2012.

Kiikkilä, O., Smolander, A., and Kitunen, V.: Degradability, molecular weight and adsorption properties of dissolved organic carbon and nitrogen leached from different types of decomposing litter, Plant Soil, 373, 787–798, https://doi.org/10.1016/j.femsec.2004.08.011, 2013.

Koehler, B., Landelius, T., Weyhenmeyer, G. A., Machida, N., and Tranvik, L. J.: Sunlight-induced carbon dioxide emissions from inland waters, Global Biogeochem. Cy., 28, 696–711, https://doi.org/10.1002/2014GB004850, 2014.

Köhler, S., Buffam, I., Jonsson, A., and Bishop, K.: Photochemical and microbial processing of stream and soil water dissolved organic matter in a boreal forested catchment in northern Sweden, Aquat. Sci., 64, 269–281, https://doi.org/10.1007/s00027-002-8071-z, 2002.

Kopáček, J., Klementova, S., and Norton S. A.: Photochemical production of ionic and particulate aluminum and iron in lakes, Environ. Sci. Technol., 39, 3656–3662, https://doi.org/10.1021/es048101a, 2005.

Kopáček, J., Marešová, M., Norton, S. A., Porcal, P., and Veselý, J.: Photochemical source of metals for sediments, Environ. Sci. Technol., 40, 4455–4459, https://doi.org/10.1021/es0600532, 2006.

Krickov, I. V., Pokrovsky, O. S., Manasypov, R. M., Lim, A., Shirokova, L. S., and Loiko, S. V.: Colloidal transport of carbon and metals by western Siberian rivers during different seasons across a permafrost gradient, Geochim. Cosmochim. Acta, 265, 221–241, https://doi.org/10.1016/j.gca.2019.08.041, 2019.

Lapierre, J.-F., Guillemette, F., Berggren, M., and del Giorgio, P. A.: Increases in terrestrially derived carbon stimulate organic carbon processing and CO_2 emissions in boreal aquatic ecosystems, Nat. Commun., 4, 2972, https://doi.org/10.1038/ncomms3972, 2013.

Larouche, J. R., Abbott, B. W., Bowden, W. B., and Jones, J. B.: The role of watershed characteristics, permafrost thaw, and wildfire on dissolved organic carbon biodegradability and water chemistry in Arctic headwater streams, Biogeosciences, 12, 4221–4233, https://doi.org/10.5194/bg-12-4221-2015, 2015.

Lau, M. P.: Linking the dissolved and particulate domain of organic carbon in inland waters. J. Geophys. Res.-Biogeosci., 126, e2021JG006266, https://doi.org/10.1029/2021JG006266, 2021.

Laurion, I. and Mladenov, N.: Dissolved organic matter photolysis in Canadian Arctic thaw ponds, Environ. Res. Lett., 8, 035026, https://doi.org/10.1088/1748-9326/8/3/035026, 2013.

Laurion, I., Massicotte, P., Mazoyer, F., Negandhi, K., and Mladenov, N.: Weak mineralization despite strong processing of dissolved organic matter in Eastern Arctic tundra ponds, Limnol. Oceanogr., 66, S47–S63, https://doi.org/10.1002/lno.11634, 2021.

Liu, F. and Wang, D.: Dissolved organic carbon concentration and biodegradability across the global rivers: A meta-analysis, Sci. Total Environ., 818, 151828, https://doi.org/10.1016/j.scitotenv.2021.151828, 2022.

Lou, T. and Xie, H.: Photochemical alteration of the molecular weight of dissolved organic matter, Chemosphere, 65, 2333–2342, https://doi.org/10.1016/j.chemosphere.2006.05.001, 2006.

Mann, P. J., Davydova, A., Zimov, N., Spencer, R. G. M., Davydov, S., Bulygina, E., Zimov, S., and Holmes, R. M.: Controls on the composition and lability of dissolved organic matter in Siberia's Kolyma River basin, J. Geophys. Res., 117, G01028, https://doi.org/10.1029/2011JG001798, 2012.

Mann, P. J., Sobczak, W. V., LaRue, M. M., Bulygina, E., Davydova, A., Vonk, J. E., Schade, J., Davydov, S., Zimov, N., Holmes, R. M., and Spencer, R. G. M.: Evidence for key enzymatic controls on metabolism of Arctic river organic matter, Global Change Biol., 20, 1089–1100, https://doi.org/10.1111/gcb.12416, 2014.

Mann, P. J., Eglinton, T. I., Mcintyre, C. P., Zimov, N., Davydova, A., Vonk, J. E., Holmes, R. M., and Spencer, R. G. M.: Utilization of ancient permafrost carbon in headwaters of Arctic fluvial networks, Nat. Commun., 6, 7856, https://doi.org/10.1038/ncomms8856, 2015.

Mazoyer, F., Laurion, I., and Rautio, M.: The dominant role of sunlight in degrading winter dissolved organic matter from a thermokarst lake in a subarctic peatland, Biogeosciences, 19, 3959–3977, https://doi.org/10.5194/bg-19-3959-2022, 2022.

Moody, C. S., Worrall, F., Evans, C. D., and Jones, T. G.: The rate of loss of dissolved organic carbon (DOC) through a catchment, J. Hydrol., 492, 139–150, https://doi.org/10.1016/j.jhydrol.2013.03.016, 2013.

Moran, M. A., Sheldon, W. M., and Zepp, R. G.: Carbon loss and optical property changes during long-term photochemical and biological degradation of estuarine dissolved organic matter, Limnol. Oceanogr., 45, 1254–1264, https://doi.org/10.4319/lo.2000.45.6.1254, 2000.

Mostofa, K. M. G., Yoshioka, T., Konohira, E., and Tanoue, E.: Photodegradation of fluorescent dissolved organic matter in river waters, Geochem. J., 41, 323–331, https://doi.org/10.2343/geochemj.41.323, 2007.

Obernosterer, I. and Benner, R.: Competition between biological and photochemical processes in the mineralization of dissolved organic carbon, Limnol. Oceanogr., 49, 117–124, https://doi.org/10.4319/lo.2004.49.1.0117, 2004.

Oleinikova, O., Drozdova, O. Y., Lapitskiy, S. A., Bychkov, A. Y., and Pokrovsky, O. S.: Dissolved organic matter degradation by sunlight coagulates organo-mineral colloids and produces low-molecular weight fraction of metals in boreal humic waters, Geochim. Cosmochim. Acta, 211, 97–114, https://doi.org/10.1016/j.gca.2017.05.023, 2017.

Oleinikova, O., Shirokova, L. S., Drozdova, O. Y., Lapitsky, S. A., and Pokrovsky, O. S.: Low biodegradability of dissolved organic matter and trace metal from subarctic waters by culturable heterotrophic bacteria, Sci. Total Environ., 618, 174–187, https://doi.org/10.1016/j.scitotenv.2017.10.340, 2018.

Payandi-Rolland, D., Shirokova, L. S., Tesfa, M., Lim, A. G., Kuzmina, D., Benezeth, P., Karlsson, J., Giesler, R., and Pokrovsky, O. S.: Dissolved organic matter biodegradation along a hydrological continuum in a discontinuous permafrost area: Case study of northern Siberia and Sweden, Sci. Total Environ., 749, 141463, https://doi.org/10.1016/j.scitotenv.2020.141463, 2020.

Peacock, M., Evans, C. D., Fenner, N., Freeman, C., Gough, R., Jones, T. G., and Lebron, I.: UV-visible absorbance spectroscopy as a proxy for peatland dissolved organic carbon (DOC) quantity and quality: considerations on wavelength and absorbance degradation, Environ. Sci. Process. Impact., 16, 10–12, https://doi.org/10.1039/c4em00108g, 2014.

Pickard, A. E., Heal, K. V., McLeod, A. R., and Dinsmore, K. J.: Temporal changes in photoreactivity of dissolved organic carbon and implications for aquatic carbon fluxes from peatlands, Biogeosciences, 14, 1793–1809, https://doi.org/10.5194/bg-14-1793-2017, 2017.

Pokrovsky, O. S., Dupré, B., and Schott, J.: Fe-Al-organic colloids control the speciation of trace elements in peat soil solutions: results of ultrafiltration and dialysis, Aquat. Geochem., 11, 241–278, https://doi.org/10.1007/s10498-004-4765-2, 2005.

Pokrovsky, O. S., Viers, J., Shirokova, L. S., Shevchenko, V. P., Filipov, A. S., and Dupré, B.: Dissolved, suspended, and colloidal fluxes of organic carbon, major and trace elements in Severnaya Dvina River and its tributary, Chem. Geol., 273, 136–149, https://doi.org/10.1016/j.chemgeo.2010.02.018, 2010.

Pokrovsky, O. S., Shirokova, L. S., Zabelina, S. A., Vorobieva, T. Ya., Moreva, O. Yu., Klimov, S. I., Chupakov, A. V., Shorina, N. V., Kokryatskaya, N. M., Audry, S., Viers, J., Zoutien, C., and Freydier, R.: Size fractionation of trace elements in a seasonally stratified boreal lakes: Control of organic matter and iron colloids, Aquat. Geochem., 18, 115–139, https://doi.org/10.1007/s10498-011-9154-z, 2012.

Pokrovsky, O. S., Manasypov, R. M., Loiko, S. V., and Shirokova, L. S.: Organic and organo-mineral colloids of discontinuous permafrost zone, Geochim. Cosmochim. Ac., 188, 1–20, https://doi.org/10.1016/j.gca.2016.05.035, 2016.

Porcal, P., Dillon, P. J., and Molot, L. A.: Photochemical production and decomposition of particulate organic carbon in a freshwater stream, Aquat. Sci., 75, 469–482, https://doi.org/10.1007/s00027-013-0293-8, 2013.

Porcal, P., Dillon, P. J., and Molot, L. A.: Interaction of extrinsic chemical factors affecting photodegradation of dissolved organic matter in aquatic ecosystems, Photochem. Photobiol. Sci., 13, 799–812, https://doi.org/10.1039/c4pp00011k, 2014.

Porcal, P., Dillon, P. J., and Molot, L. A.: Temperature dependence of photodegradation of dissolved organic matter to dissolved inorganic carbon and particulate organic carbon, Plos ONE, 10, e0128884, https://doi.org/10.1371/journal.pone.0128884, 2015.

Prijac, A., Gandois, L., Jeanneau, L., Taillardat, P., and Garneau, M.: Dissolved organic matter concentration and composition discontinuity at the peat–pool interface in a boreal peatland, Biogeosciences, 19, 4571–4588, https://doi.org/10.5194/bg-19-4571-2022, 2022.

Raudina, T. V., Loiko, S., Kuzmina, D. M., Shirokova, L. S., Kulizhsky, S. P., Golovatskaya, E. A., and Pokrovsky, O. S.: Colloidal organic carbon and trace elements in peat porewaters across a permafrost gradient in Western Siberia, Geoderma 390, 114971, https://doi.org/10.1016/j.geoderma.2021.114971, 2021.

Raudina, T. V., Smirnov, S. V., Luschaeva, I. V., Kulizhskiy, S. P., Golovatskaya, E. A., Shirokova, L. S., and Pokrovsky, O. S.: Seasonal and spatial variations of dissolved organic matter biodegradation along the aquatic continuum in the southern

taiga bog complex, Western Siberia, Water (MDPI), 14, 3969, https://doi.org/10.3390/w1423396, 2022.

Roehm, C. L., Giesler, R., and Karlsson, J.: Bioavailability of terrestrial organic carbon to lake bacteria: The case of a degrading subarctic permafrost mire complex, J. Geophys. Res., 114, G03006, https://doi.org/10.1029/2008JG000863, 2009.

Rosset, T., Binet, S., Rigal, F., and Gandois, L.: Peatland dissolved organic carbon export to surface waters: Global significance and effects of anthropogenic disturbance, Geophys. Res. Lett., 49, e2021GL096616, https://doi.org/10.1029/2021GL096616, 2022.

Selvam, B. P., Lapierre, J.-F., Guillemette, F., Voigt, C., Lamprecht, R. E., Biasi, C., Christensen, T. R., Martikainen P. J., and Berggren, M.: Degradation potentials of dissolved organic carbon (DOC) from thawed permafrost peat, Sci. Rep., 7, 45811, https://doi.org/10.1038/srep45811, 2016.

Serikova, S., Pokrovsky, O. S., Ala-aho, P., Kazantsev, V., Kirpotin, S. N. Kopysov, S. G., Krickov, I. V., Laudon, H., Manasypov, R. M., Shirokova, L. S., Sousby, C., Tetzlaff, D., and Karlsson, J.: High riverine CO_2 emissions at the permafrost boundary of Western Siberia, Nat. Geosci., 11, 825–829, https://doi.org/10.1038/s41561-018-0218-1, 2018.

Serikova, S., Pokrovsky, O. S., Laudon, H., Krickov, I. V., Lim, A. G., Manasypov, R. M., and Karlsson, J.: C emissions from lakes across permafrost gradient of Western Siberia, Nat. Commun., 10, 1552, https://doi.org/10.1038/s41467-019-09592-1, 2019.

Shirokova, L. S., Bredoire, R., Rolls, J. L., and Pokrovsky, O. S.: Moss and peat leachate degradability by heterotrophic bacteria: fate of organic carbon and trace metals, Geomicrobiol. J., 34, 641–655, https://doi.org/10.1080/01490451.2015.1111470, 2017a.

Shirokova, L. S., Chupakova, A. A., Chupakov, A. V., and Pokrovsky, O. S.: Transformation of dissolved organic matter and related trace elements in the mouth zone of the largest European Arctic river: experimental modeling, Inland Waters, 7, 272–282, https://doi.org/10.6084/m9.figshare.5387686, 2017b.

Shirokova, L. S., Labouret, J., Gurge, M., Gerard, E., Zabelina, S. A., Ivanova, I. S., Pokrovsky, O. S.: Impact of cyanobacterial associate and heterotrophic bacteria on dissolved organic carbon and metal in moss and peat leachate: application to permafrost thaw in aquatic environments, Aquat. Geochem., 23, 331–358, https://doi.org/10.1007/s10498-017-9325-7, 2017c.

Shirokova, L. S., Chupakov, A. V., Zabelina, S. A., Neverova, N. V., Payandi-Rolland, D., Causserand, C., Karlsson, J., and Pokrovsky, O. S.: Humic surface waters of frozen peat bogs (permafrost zone) are highly resistant to bio- and photodegradation, Biogeosciences, 16, 2511–2526, https://doi.org/10.5194/bg-16-2511-2019, 2019.

Shirokova, L. S., Chupakov, A. V., Ivanova, I. S., Moreva, O. Y., Zabelina, S. A., Shutskiy, N. A., Loiko S. V., and Pokrovsky, O. S.: Lichen, moss and peat control of C, nutrient and trace metal regime in lakes of permafrost peatlands, Sci. Total Environ., 782, 146737, https://doi.org/10.1016/j.scitotenv.2021.146737, 2021.

Spencer, R. G. M., Mann, P. J., Dittmar, T., Eglinton, T. I., McIntyre, C., Holmes, R. M., Zimov, N., and Stubbins, A.: Detecting the signature of permafrost thaw in Arctic rivers, Geophys. Res. Lett., 42, 2830–2835, https://doi.org/10.1002/2015GL063498, 2015.

Stubbins, A., Spencer, R. G., Chen, H., Hatcher, P. G., Mopper, K. W., Hernes, P. J., Mwamba, V., Mangangu, A. M., Wabakanghanzi, J. N., and Six, J.: Illuminated darkness: Molecular signatures of Congo River dissolved organic matter and its photochemical alteration as revealed by ultrahigh precision mass spectrometry, Limnol. Oceanogr., 55, 1467–1477, https://doi.org/10.4319/lo.2010.55.4.1467, 2010.

Stutter, M. I., Richards, S., and Dawson, J. J. C.: Biodegradability of natural dissolved organic matter collected from a UK moorland stream, Water Res., 47, 1169–1180, https://doi.org/10.1016/j.watres.2012.11.035, 2013.

Sulzberger, B., Austin, A. T., Cory, R. M., Zepp, R. G., and Paul, N. D.: Solar UV radiation in a changing world: roles of cryosphere-land-water-atmosphere interfaces in global biogeochemical cycles, Photochem. Photobiol. Sci., 18, 747–774, https://doi.org/10.1039/c8pp90063a, 2019.

Taillardat, P., Bodmer, P., Deblois, C. P., Ponçot, A., Prijac, A., Riahi, K., Gandois, L., del Giorgio, P. A., Bourgault, M. A., Tremblay, A., and Garneau, M.: Carbon dioxide and methane dynamics in a peatland headwater stream: Origins, processes and implications, J. Geophys. Res.-Biogeosci., 127, e2022JG006855, https://doi.org/10.1029/2022JG006855, 2022.

Textor, S. R., Guillemette, F., Zito, P. A., and Spencer, R. G. M.: An assessment of dissolved organic carbon biodegradability and priming in blackwater systems, J. Geophys. Res.-Biogeosci., 123, 2998–3015, https://doi.org/10.1029/2018JG004470, 2018.

Tranvik, L. J., Downing, J. A., Cotner, J. B., Loiselle, S. A., Striegl, R. G., Ballatore, T. J., Dillon, P., Finlay, K., Fortino, K., Knoll, L. B., Kortelainen, P. L., Kutser, T., Larsen, S., Laurion, I., Leech, D. M., McCallister, S. L., McKnight, D. M., Melack, J. M., Overholt, E., Porter, J. A., Prairie, Y., Renwick, W. H., Roland, F., Sherman, B. S., Schindler, D. W., Sobek, S., Tremblay, A., Vanni, M. J., Verschoor, A. M., von Wachenfeldt, E., and Weyhenmeyer, G. A.: Lakes and reservoirs as regulators of carbon cycling and climate, Limnol. Oceanogr., 54, 2298–2314, https://doi.org/10.4319/lo.2009.54.6_part_2.2298, 2009.

Vachon, D., Lapierre, J., and del Giorgio, P. A.: Seasonality of photochemical dissolved organic carbon mineralization and its relative contribution to pelagic CO_2 production in northern lakes, J. Geophys. Res.-Biogeo., 121, 864–878, https://doi.org/10.1002/2015JG003244, 2016.

Vachon, D., Solomon, C. T., and del Giorgio, P. A.: Reconstructing the seasonal dynamics and relative contribution of the major processes sustaining CO_2 emissions in northern lakes, Limnol. Oceanogr., 62, 706–722, https://doi.org/10.1002/lno.10454, 2017.

Vähätalo, A. V., Salkinoja-Salonen, M., Taalas, P., and Salonen, K.: Spectrum of the quantum yield for photochemical mineralization of dissolved organic carbon in a humic lake, Limnol. Oceanogr., 45, 664–676, https://doi.org/10.4319/lo.2000.45.3.0664, 2000.

Vähätalo, A. V. and Wetzel, R. G.: Photochemical and microbial decomposition of chromophoric dissolved organic matter during long (months-years) exposures, Mar. Chem., 89, 313–326, https://doi.org/10.1016/j.marchem.2004.03.010, 2004.

Vähätalo, A. V., Salonen, K., Münster, U., Järvinen, M., and Wetzel, R. G.: Photochemical transformation of allochthonous organic matter provides bioavailable nutrients in a humic lake, Acta Hydrobiol., 156, 287–314, https://doi.org/10.1127/0003-9136/2003/0156-0287, 2003.

Vasyukova, E., Pokrovsky, O. S., Viers, J., Oliva, P., Dupré, B., Martin, F., and Candaudap, F.: Trace elements in organic- and iron-

rich surficial fluids of boreal zone: Assessing colloidal forms via dialysis and ultrafiltration, Geochim. Cosmochim. Acta, 74, 449–468, https://doi.org/10.1016/j.crte.2012.08.003, 2010.

Vonk, J. E., Tank, S. E., Mann, P. J., Spencer, R. G. M., Treat, C. C., Striegl, R. G., Abbott, B. W., and Wickland, K. P.: Biodegradability of dissolved organic carbon in permafrost soils and aquatic systems: a meta-analysis, Biogeosciences, 12, 6915–6930, https://doi.org/10.5194/bg-12-6915-2015, 2015.

Ward, C. P., Nalven, S. G., Crump, B. C., Kling, G. W., and Cory, R. M.: Photochemical alteration of organic carbon draining permafrost soils shifts microbial metabolic pathways and stimulates respiration, Nat. Commun., 8, 772, https://doi.org/10.1038/s41467-017-00759-2, 2017.

Wauthy, M., Rautio, M., Christoffersen, K. S., Forsstrom, L., Laurion, I., Mariash, H. L., Peura, S., and Vincent, W. F.: Increasing dominance of terrigenous organic matter in circumpolar freshwaters due to permafrost thaw, Limnol. Oceanogr. Lett., 3, 2018, 186–198, https://doi.org/10.1002/lol2.10063, 2012.

Weishaar, J. L., Aiken, G. R., Bergamaschi, B. A., Fram, M. S., Fujii, R., and Mopper, K.: Evaluation of specific ultraviolet absorbance as an indicator of the chemical composition and reactivity of dissolved organic carbon, Environ. Sci. Technol., 37, 4702–4708, https://doi.org/10.1021/es030360x, 2003.

Wickland, K. P., Aiken G. R., Butler K., Dornblaser M. M., Spencer R. G. M., and Striegl R. G.: Biodegradability of dissolved organic carbon in the Yukon River and its tributaries: seasonality and importance of inorganic nitrogen. Global Biogeochem. Cy., 26, 2012gb004342, https://doi.org/10.1029/2012GB004342, 2012.

Wilske, C., Herzsprung, P., Lechtenfeld, O. J., Kamjunke, N., and von Tümpling, W.: Photochemically induced changes of dissolved organic matter in a humic-rich and forested stream, Water, 12, 331, https://doi.org/10.3390/w12020331, 2020.

Winter, A. R., Fish, T. A. E., Playle, R. C., Smith, D. S., and Curtis, P. J.: Photodegradation of natural organic matter from diverse freshwater sources, Aquat. Toxicol., 84, 215–222, https://doi.org/10.1016/j.aquatox.2007.04.014, 2007.

Zabelina, S. A., Shirokova, L. S., Klimov, S. I., Chupakov, A. V., Lim, A. G., Polishchuk, Y. M., Polishchuk, V. Y., Bogdanov, A. N., Muratov, I. N., Guerin, F., Karlsson, J., and Pokrovsky, O. S.: Carbon emission from thermokarst lakes in NE European tundra, Limnol. Oceanogr., 66, S216–S230, https://doi.org/10.1002/lno.11560, 2021.